1-1-2002

Using diffuse idiopathic skeletal hyperostosis to determine age at death

Jennifer Elizabeth Riddle
University of Nevada, Las Vegas

NOTE TO USERS

Page(s) not included in the original manuscript and are unavailable from the author or university. The manuscript was scanned as received.

missing vita page 127

This reproduction is the best copy available.

UMI®

USING DIFFUSE IDIOPATHIC SKELETAL HYPEROSTOSIS TO DETERMINE AGE AT DEATH

by

Jennifer E. Riddle

Bachelor of Arts
University of North Carolina at Greensboro
1999

A thesis submitted in partial fulfillment
of the requirements for the

Master of Arts Degree
Department of Anthropology
College of Liberal Arts

Graduate College
University of Nevada, Las Vegas
December 2002

ProQuest Information and Learning Company
300 North Zeeb Road
P.O. Box 1346
Ann Arbor, MI 48106-1346

UNLV
UNIVERSITY OF NEVADA, LAS VEGAS

Thesis Approval

The Graduate College
University of Nevada, Las Vegas

August 23, 2002

The Thesis prepared by

Jennifer Elizabeth Riddle

Entitled

Using Diffuse Idiopathic Skeletal Hyperostosis to Determine Age at Death

is approved in partial fulfillment of the requirements for the degree of

Master of Arts, Anthropology

Examination Committee Chair

Dean of the Graduate College

Examination Committee Member

Examination Committee Member

Graduate College Faculty Representative

ABSTRACT

Using Diffuse Idiopathic Skeletal Hyperostosis to Determine Age at Death

by

Jennifer E. Riddle

Dr. Bernardo Arriaza, Examination Committee Chair
Professor of Anthropology
University of Nevada, Las Vegas

This research took an age-related condition, diffuse idiopathic skeletal hyperostosis (DISH) and used it to create a new technique for estimating the age at death of older human skeletal remains (age $\geq$ 40). Diffuse idiopathic skeletal hyperostosis is a condition characterized spinally by ossification of the anterior longitudinal ligament resulting in fusion of vertebrae; and extraspinally by enthesopathies, ossification at sites of ligament or muscle attachments. Using the Terry Collection, housed at the Smithsonian Institution, National Museum of Natural History, 1728 human skeletons of known age at death were analyzed looking for evidence of spinal DISH. Found in 94 individuals, the level of DISH was scored and measured. The measurements taken from these individuals were correlated to age at death using Pearson product-moment correlation coefficient tests.

Regression equations were created based on the correlations and produced R-square values of 52% for incipient/mild males, 41% for moderate/severe males, 85% for incipient/mild females and 91% for moderate/severe females, meaning that DISH is a good indicator of age at death, especially in females. This research is unique in that most techniques for age estimation reach their maximum at about 60 years, while the DISH-based technique presented in this thesis can reliably age people into their early 100s. Thus the results of this research make a valuable contribution to the field of physical anthropology.

LIST OF FIGURES

LIST OF TABLES

ACKNOWLEDGMENTS

I would like to thank the following: the Smithsonian Institution, National Museum of Natural History, particularly Dr. David Hunt, for allowing me access to the Terry Collection. The Department of Anthropology and Ethnic Studies (UNLV) for its munificent Edwards and Olswang Grant. My committee, Dr. Bernardo Arriaza, Chair, Dr. Vicki Cassman, Dr. Jennifer Thompson and Dr. Roberta Williams for their support and guidance throughout my graduate career.

Finally, I would like to thank my aunt and uncle, Donna and David Hibbard, for their very gracious hospitality and generosity when their niece paid them a two month visit. Thanks should also go to my parents, Thomas and Mary Riddle, my brother, Andrew Riddle, and my sister-in-law, Tara Riddle, for enduring a three year conversation about DISH.

TABLE OF CONTENTS

CHAPTER 1

INTRODUCTION

From dinosaurs (Rothschild, 1988) to humans, diffuse idiopathic skeletal hyperostosis is a condition that has spanned millennia (Rothschild, 1988; Arriaza et al., 1993). While the etiology of diffuse idiopathic skeletal hyperostosis (DISH) is unclear (Forestier and Rotes-Querol, 1950; Hajkova et al., 1965; Rothschild, 1988), the condition, nonetheless, has the potential to tell researchers much about the individual who had it. Previous research has found that the prevalence of DISH increases with age (Julkunen et al., 1975; Arriaza, 1993; Maat et al., 1995). However, while it is known that older people are more likely to have DISH, there has been no systematic study attempting to determine biological age based on the severity of DISH observed in the skeleton. Therefore, the purpose of this research is to create a system by which the biological age of an individual can be estimated based on the level of DISH seen in the skeleton.

DISH: an introduction

Diffuse idiopathic skeletal hyperostosis is characterized by enthesopathies, bony spurs occurring at points of muscle insertions (Benjamin et al., 2000), that can happen anywhere in the body (Schwartz, 1995). However, DISH usually occurs in the vertebral column with the ossification of the anterior longitudinal ligament (ALL) (Crubézy, 1990; Schwartz, 1995). The ossification of the ALL is often said to give the appearance of "dripping candle wax" (Forestier and Rotes-Querol, 1950). Typically, only the right side of the anterior longitudinal ligament ossifies; researchers believe the left side does not ossify due to the pulsation of the aorta (Aufderheide and Rodríguez-Martín, 1998; Fairgrieve, 1999). Despite the ossification of the ALL, an important distinguishing characteristic of DISH is the maintenance of intervertebral disc space and normal zygoapophyseal joints (Resnick et al. 1975; Arriaza et al., 1993).

Diffuse idiopathic skeletal hyperostosis most often occurs in the thoracic portion of the vertebral column; however, it can occur in the cervical and lumbar regions as well (Resnick et al. 1975; Resnick and Niwayama, 1976; Rogers et al., 1987; Arriaza, 1993). Because DISH usually occurs in the thoracic vertebrae, individuals with DISH typically do not loose spinal flexibility. In fact, some workers believe DISH is an advantageous adaptation stating the condition provides additional spinal

support and helps to prevent neuroforaminal narrowing (Rothschild, 1988; Rothschild and Woods, 1991).

The antiquity of DISH in the Old World is quite extensive. As has been pointed out, Rothschild (1988) has found evidence of DISH throughout the fossil record. Lagier (1989) has also found numerous incidences of DISH in multiple species. In hominids, DISH has been found in the Shanidar 1 Neanderthal, which is estimated to date from 73,000 to 40,000 years BP (Crubézy and Trinkaus, 1992). In fully modern humans, DISH has been found in ancient Egyptian mummies (Forestier and Lagier, 1971). Arriaza et al. (1993) have found DISH in ancient Nubians dating back two thousand years. In the New World, Arriaza (1993) has found DISH in northern Chilean populations dating to four thousand years ago. Studies suggest, however, that the incidence of DISH has grown with the rise in agropastorialism (Arriaza, 1993).

The presence of DISH in ancient populations as well as more modern ones makes this research useful because previous studies indicate a high likelihood that a certain percentage of any population under study by a given worker will have DISH. Thus, the ability to age older individuals by the severity of DISH gives anthropologists a new tool that is applicable in multiple populations.

The problem

Despite many years of being in the literature, there is much about DISH that is unresolved. For instance, DISH has been associated with age but only in a general way. Researchers have noticed trends, such as higher rates of DISH in older individuals, but have not taken the relationship further. This research is unique in that it establishes correlations between the amount of DISH ossification in the skeleton and age at death. It then uses the correlations to create regression equations that can be used to predict age based on DISH.

In addition to problems of quantifying the relationship between DISH and age, there is also the rather cumbersome problem of no uniform scoring system for the condition. Most scoring systems currently in the literature never go beyond simple "presence/absence." However, DISH can affect just one vertebra or multiple vertebrae. The ossification can be thick and pronounced or it can be a mere spur. If researchers want to compare DISH in different populations then there must be a more detailed, universally accepted method for scoring DISH.

Hypothesis

The hypothesis underlying this thesis is that the amount of DISH ossification in the skeleton will correlate quite well to an age at death independent of biological affinity. If this hypothesis is correct, then regression equations will be able to predict age at death based on the

level of DISH in the skeleton. The hypothesis is a logical one given that DISH is not found before age 40 (Rogers et al., 1985; Crubézy, 1990; Aufderheide and Rodríguez-Martin, 1998), thereby establishing a baseline age for people with DISH. For example, even before the relationship between DISH and age has been more precisely defined by this thesis, a researcher can confidently state that an individual with DISH is at least 40 years old. If DISH ossification does not take place until age 40, then it would make sense that individuals exhibiting copious amounts of DISH ossification would be much older than age 40 because it would take time for the ossification to develop. Further, if DISH ossification progresses at a predictable rate then that rate should be measurable and should accurately predict age at death.

Diffuse idiopathic skeletal hyperostosis is a good choice for creating an aging technique not only for the reasons already discussed, but also because it is arguably not a pathological condition, instead it can be seen as a useful adaptation that gives structural support to the spine and prevents neuroforamenal narrowing (Rothschild, 1988; Rothschild and Woods, 1991). Finally, according to current clinical studies, DISH is found in 15 to 20 percent of modern populations (Resnick, 1985; Rothschild, 1985; Aufderheide and Rodríguez-Martin, 1998), thus making a DISH based aging method useful in many forensic settings.

The chapters

The next chapter in this thesis gives a detailed literature review of DISH starting with the historical names surrounding the condition. It explains the difference between DISH seen in the spine and DISH seen in other parts of the body and then presents a comprehensive differential diagnosis of the condition.

Chapter Three explains the methodology used in this research. It describes the population from which the data were collected, the previous study from which the scoring system was devised, and the various measurements taken from the skeletons used in this research. It then describes the statistical tests used in the data analyses, chi square, Pearson r, and regression, and why they were appropriate.

Chapter Four focuses on the results of the analyses, explaining what the statistical tests revealed. Chi square showed that males and females are differentially affected by DISH with a significance of $X^2 = 12.12$; $p < 0.05$. However, there were no significant differences between biological affinity groups ($X^2 = 4.67$; $p > 0.05$). Pearson's r reveals many correlations between various areas of DISH ossification seen in the skeleton and age at death. Finally, Chapter Four details the regression equations created for each category of DISH (incipient/mild females, incipient/mild males, moderate/severe females, moderate/severe males) and shows the R-square values and whole model probabilities for each equation.

The final chapter discusses what the results mean. It points out that the regression equations created for females are more reliable than those created for males, suggesting this technique may be more useful for females. It acknowledges that the sample size within each DISH category became smaller than a definitive statistical test would ideally have and suggests that this study be considered an exploratory analysis of the relationship between DISH and age at death. Chapter Five explains how the preliminary results created by this thesis warrant further research within various populations (i.e. populations of different biological affinities, archaeological populations) to see if the regression equations need to be adjusted by population and to increase the sample size on which the equations are based.

CHAPTER 2

LITERATURE REVIEW

DISH in an historical literary context

The literary history of diffuse idiopathic skeletal hyperostosis is a long and varied one. The earliest reports of the disease come from Meyer and Forester, who in 1938, wrote about a patient with ossification on the right side of his vertebral column. Meyer and Forester called the condition "moniliform hyperostosis" (Utsinger, 1985). The Meyer and Forester report was quickly followed by Oppenheimer's 1942 study in which he described a case of ossification of the anterior longitudinal ligament; he called this spinal pathology "spondylitis ossificans ligamentosa" (Oppenheimer, 1942). As the years went by, many researchers studied the phenomenon and attempted to create a name that more accurately described the condition. For instance, in 1950 Forestier and Rotes-Querol wrote their seminal piece on the condition, focusing on radiology and the new information it could convey. Realizing that the condition affected only the elderly, the two renamed it "senile ankylosing hyperostosis of the spine" (Forestier and Rotes-Querol, 1950).

In 1975 Resnick et al. recognized that the skeletal ossification affected not only the anterior longitudinal ligament of the spine, but also many other areas of muscle insertion throughout the skeleton. It was at that point that Resnick et al. (1975) proposed the name "diffuse idiopathic skeletal hyperostosis," arguing that it was more descriptive of the condition and that it emphasized the fact that hyperostosis was not confined to the vertebral column (Resnick et al., 1975).

While the literary history of DISH and the many incarnations of its name might seem an inconsequential point at this time, it is actually quite important. No complete research into the condition can be done without knowing the historical names lest one risk missing critical information because one did not recognize "spondylitis ossificans ligamentosa" as an early version of DISH. Also, many researchers believe that the full extent of DISH in the archaeological record is not known because many cases of DISH have been misdiagnosed (Rogers et al., 1985; Crubézy, 1990; Crubézy and Trinkaus, 1992; Suzuki et al., 1993). Table 1 lists some of the more common names often used interchangeably with DISH.

As has been implied in the discussion of the various names given to DISH, diffuse idiopathic skeletal hyperostosis can impact the entire postcranial skeleton – not just the spine. However, for the purposes of this discussion, it is easier to break the postcranial skeleton into two

parts using Resnick et al.'s (1975) terms: spinal and extraspinal manifestations.

TABLE 1. Common names used interchangeably with DISH[1]

Common Synonyms
Ankylosing hyperostosis
Ankylosing hyperostosis of Forestier and Rotes-Querol
Ankylosing vertebral hyperostosis
Forestier's disease
Moniliform hyperostosis
Senile ankylosing hyperostosis of the spine
Spondylitis ossificans ligmentosa

[1]After: Utsinger, 1985; Arriaza et al., 1993

Spinal manifestations of DISH

Number of vertebrae that must fuse. It is generally agreed that spinal manifestations of DISH are the most diagnostic aspects of the condition (Resnick, 1985; Utsinger, 1985; Crubézy and Trinkaus, 1992). However, there is disagreement over the number of consecutive vertebrae that must be fused by ossification of the anterior longitudinal ligament before an accurate diagnosis of DISH can be made. Hukuda et al. (2000) use a definition that requires only the tip of the ossification from one vertebra to reach the adjacent vertebrae. Julkunen et al. (1975) state there must be fusion of at least two contiguous vertebrae in two separate areas of

the spine. Rogers et al. (1987) argue that, at least in the clinical setting, a diagnosis of DISH can be made when three or more consecutive vertebrae are fused. The classic diagnostic criteria defined by Resnick and Niwayama (1976), and reinforced by Littlejohn et al. (1981) and Aufderheide and Rodríguez-Martín (1998), states there must be fusion of at least four consecutive vertebrae. Figure 1 shows a classic case of DISH with the fusion of multiple vertebrae.

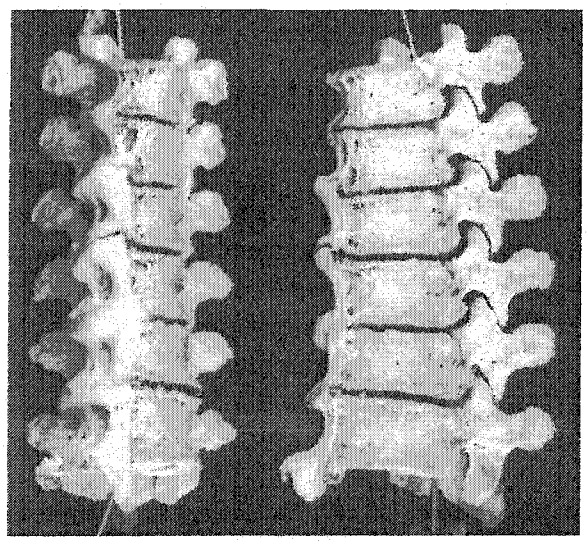

Fig. 1. Smithsonian Institution, Terry Collection #842: Male, white, age 73: A classic case of DISH with the fusion of six contiguous vertebrae.

In 1985 Utsinger dealt with the lack of uniformity in the number of consecutively fused vertebrae that must be present to call a condition DISH by establishing a scoring system of sorts that incorporated the

various viewpoints. He had three categories: definite, probable, and possible. Definite DISH had fusion of at least four consecutive vertebrae; probable and possible categories involved the fusion of at least two consecutive vertebrae in combination with various extraspinal ossification. This researcher agrees with Hukuda et al. (2000) in that only spurs need be present to diagnose DISH. This thesis follows a scoring system proposed by Arriaza (2000), which will be described in Chapter Three.

Characteristics of the ossification. Despite rampant disagreement over the number of fused vertebrae needed to justify calling spinal hyperostosis DISH, everyone agrees that it is important that most of the intervertebral disc space be maintained (Forestier and Lagier, 1971; Resnick and Niwayama, 1976; Utsinger, 1985; Arriaza, 1993; Aufderheide and Rodriguez-Martín, 1998).

Along with maintaining intervertebral disk space, the ossification seen in DISH is predominately right sided and has been described as looking like "dripping candle wax" (Forestier and Rotes-Querol, 1950). While acknowledging the hyperostosis is usually right sided, Rogers et al. (1987) believe there is a higher likelihood of the ossification being bilateral if it is located in either the cervical or lumbar regions of the spine. Researchers believe the left side of the vertebral column is not usually affected by DISH because the constantly pulsating aorta does not

allow the ligament to ossify (Hájková et al., 1965; Fairgrieve, 1999). If true, it might give weight to Oppenheimer's (1942) speculation that the anterior longitudinal ligament ossifies due to lack of movement and use.

In addition to often being right sided, DISH ossification is usually located in the thoracic section of the vertebral column (Resnick, 1985; Rothschild, 1988). While it is unknown why the thoracic section is most often affected, it may be due in part to how the anterior longitudinal ligament (ALL) is constructed. As Resnick and Niwayama (1976) explain, the ALL is a long ligament that reaches from the skull to the sacrum. It is narrow in the cervical region of the vertebrae and becomes progressively wider in the thoracic area until it covers nearly the entire anterolateral surface of the thoracic vertebrae. As it descends to the lumbar region, it narrows once again. The ALL forms part of the vertebral periosteum in places where it actually attaches to the anterior surface of the vertebrae (Resnick and Niwayama, 1976). Given that humans have the least range of motion in the thoracic section of the vertebral column and that the ALL is widest in the thoracic area, it is possible that Oppenheimer's (1942) postulation of inactivity leading to ALL ossification, coupled with the relatively large width of the ALL, could explain the higher rates of ossification in the thoracic region. Also, during flexion and extension the thoracic area moves as a block while the lumbar vertebrae have more individual movement.

Blocks of ossification. Each segment of ossification along the vertebral column is referred to as a block. It is possible for the ossification to break postmortemly; however, it is still considered one block. For there to be more than one block, the ossification must have obvious starting and ending points in more than one area of the vertebral column. Figure 2 illustrates this point by showing a vertebral column with one block of broken ossification.

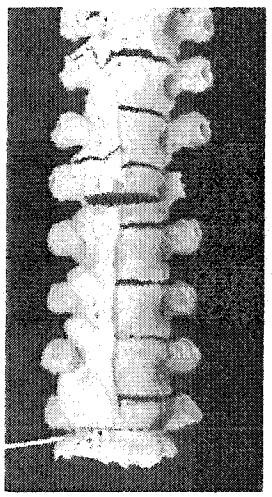

Fig. 2. Smithsonian Institution, Terry Collection #1069: Female, white, age 70: Spine with one block of broken ossification.

Summary of spinal DISH criteria. In classic DISH, there is fusion of four contiguous vertebrae. The ossification is predominantly right sided and is usually found in the thoracic section of the vertebral column. Intervertebral disc space is maintained and apophyseal joints are spared. Typical DISH cases are males over the age of 40, as DISH is a condition

usually reserved for the elderly and affects males more than females (Julkunen et al., 1975; Resnick and Niwayama, 1976; Utsinger, 1985; Arriaza, 1993; Auferdheide and Rodríguez-Martín, 1998).

Differential diagnosis of spinal conditions

It is important to recognize that there are other spinal conditions that may be confused with DISH, and that the ability to distinguish DISH from other spinal pathologies is a vital skill. Pathologies that are most likely to cause confusion are spondylosis deformans/vertebral osteophytes and the suite of seronegative spondyloarthropathies because they all involve fusion of the vertebral column (Rothschild and Woods, 1989; Arriaza, 1993).

Spondylosis deformans. Spondylosis deformans (SD) is a degenerative non-inflammatory condition that affects all areas of the vertebral column (Mann and Murphy, 1990; Kahl and Smith, 2000). The condition is characterized by osteophytes, abnormal bone growths that in their extreme form can create bony bridges between vertebrae (Chapman, 1972). Generally the lumbar area is the most affected segment followed by the thoracic and cervical regions; however, vertebral segments most affected by spondylosis deformans vary according to population (Bridges, 1994). For example, Bridges (1994) found that Koniag Eskimos have higher SD rates in the thoracic region, and individuals in the Terry

collection have higher rates in the cervical area. Kahl and Smith (2000) confirmed Bridges' assertion of population differences when they too found different rates of SD in various segments of the spine. However, despite differences in segmental SD rates, there are areas within each segment that are more prone to SD than others. These are the spinal segments of maximum curvature and thus bear most of the weight of bipedalism. The areas of maximum curvature are: C4-C7 in the cervical region; T6-T10 in the thoracic region; and L2-L5 in the lumbar region (Kahl and Smith, 2000).

The etiology of spondylosis deformans is not clearly understood; however, it seems to be both a product of aging and of chronic heavy load bearing stress (Schmorl, 1971; Chapman, 1972; Merbs, 1983; Bridges, 1994; Kahl and Smith, 2000). Spondylosis deformans is quite common and affects people who are at least 30 years of age, but is more prevalent in older people (Ortner and Putschar, 1985; Resnick and Niwayama, 1995). The male to female ratio in SD is under debate with some researchers declaring that males are affected much more than females (Mann and Murphy, 1990). Others state the overall rates between males and females are the same, it is just the age of onset that differs (Schmorl, 1971). Still others say the ratio is practically equal (Kahl and Smith, 2000).

In 1972 Chapman devised a scoring system for spondylosis deformans that consisted of five stages. The stages ranged from minor

lipping at the vertebral margins to actual ankylosis or fusion of the vertebrae. When fusion occurs it is often difficult to distinguish SD from diffuse idiopathic skeletal hyperostosis. However, in SD, there is a loss of intervertebral disc space (Rothschild, 1988; Kahl and Smith, 2000). There is no loss of disc space in DISH. Also, while fusion in SD can be right sided, it is not exclusively so. The photographs Chapman (1972) used to define her scoring system show spondylosis deformans around the entire vertebral margin – not just on one side. Figure 3 shows two examples of spondylosis deformans.

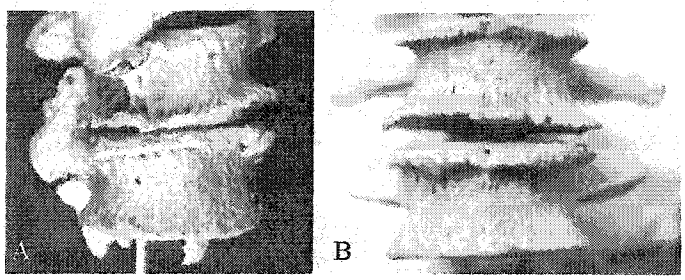

Fig. 3. **a:** Smithsonian Institution, Terry Collection #788: Male, black age 65: Lumbar spondylosis deformans. **b:** Smithsonian Institution, Terry Collection #1286: Male, white age 50: Lumbar spondylosis deformans.

Seronegative spondyloarthropathies. The seronegative spondyloarthropathies (SNS) are a type of arthritis characterized by vertebral ankylosing, sacroiliac fusion, and various other extraspinal bone changes (Rothschild and Woods, 1992; Blondiaux et al., 1997;

Rothschild et al., 1999). There are five kinds of seronegative spondyloarthropathies: ankylosing spondylitis, Reiter's syndrome, psoriatic arthritis, arthritis associated with idiopathic inflammatory bowel disease and undifferentiated seronegative spondyloarthropathy (Rothschild and Woods, 1992; Gratocós et al., 1999; Rothschild et al., 1999; Martínez-Borra et al., 2000; Said-Nahal et al., 2000). While the etiology of the seronegative spondyloarthropathies is unclear (Bass et al., 1974; Bywaters, 1983; Woodrow, 1985; Martínez-Borra et al., 2000; Said-Nahal et al., 2000), the justification for grouping these five disorders together is twofold: first, the disorders manifest similar clinical symptoms when a person is first affected with the disease. Second, the diseases run in families leading researchers to believe there is a common genetic link between the conditions (Martínez-Borra et al., 2000; Said-Nahal et al., 2000).

Family studies and other clinical observations alerted researchers to the presence of HLA-B27 among those suffering from seronegative spondyloarthropathies. HLA-B27 is a class I major histocompatability (MHC) allele found on the HLA-B locus (Hammer et al., 1990). Not everyone with seronegative spondyloarthropathies has the HLA-B27 allele; however, studies have shown a strong link between the allele and the development of seronegative spondyloarthropathies (Hammer et al., 1990; Ekman et al., 2000; Martínez-Borra et al., 2000; Said-Nahal et al., 2000)).

In an effort to more fully establish HLA-B27 as the genetic, causative agent for seronegative spondyloarthropathies, Hammer et al. (1990) turned to transgenic rats. They found that most of the transgenic rats expressing the HLA-B27 allele developed at least one seronegative spondyloarthropathy. However, while they did establish a link between HLA-B27 and seronegative spondyloarthropathies, they acknowledged that their study left open the possibility that another class I MHC gene might also cause seronegative spondyloarthropathies (Hammer et al., 1990).

Logically there must be another causative factor in the development of seronegative spondyloarthropathies because no one has reported 100% of those with the diseases as HLA-B27 positive. In fact, more recent studies show that the percentage of HLA-B27 positive people with seronegative spondyloarthropathies varies with ethnicity and the type of seronegative spondyloarthropathy the person has (Martínez-Borra, 2000; Vittecoq et al., 2000). A mere literature review supports the idea that ethnicity affects HLA-B27 status.

Not only do HLA-B27 rates vary with ethnicity, the latest research has revealed the presence of other class I MHCs such as HLA-B39 and HLA-B35 in those with seronegative spondyloarthropathies (Sobao et al., 1999; Said-Nahal et al., 2000). Newer animal studies have suggested the presence of multiple genes in seronegative spondyloarthropathy susceptibility, and twin and family studies have suggested that there

must be a triggering device that determines who among the HLA-B27 positive people will develop seronegative spondyloarthropathies (Weinreich et al., 1995; Ekman et al., 2000; Martínez-Borra, 2000). Thus for now, researchers can only conclude that the HLA-B27 allele drastically increases a person's susceptibility to seronegative spondyloarthropathies.

Despite not knowing the exact mechanics behind contracting a seronegative spondyloarthropathy, the skeletal manifestations of the diseases are well documented. The seronegative spondyloarthropathies often result in vertebral ossification that can be confused with DISH. Seronegative spondyloarthropathies that most look like DISH, and thus are to be considered here, are ankylosing spondylitis, Reiter's syndrome, and psoriatic arthritis.

Ankylosing spondylitis. As earlier stated, the exact etiology of the seronegative spondyloarthropathies, and by extension ankylosing spondylitis (AS), is unclear. Despite a lack of knowledge surrounding the cause of AS, the clinical features of the disease are well known. Ankylosing spondylitis often begins by fusing the sacroiliac joint (Arnett, 1997; Brandt et al., 2000; François et al., 2000). In fact sacroilitis is often considered the cornerstone of an AS diagnosis (Van der Linden et al., 1984; Dougados et al., 1991).

In its early active stages AS can cause the sufferer to loose significant bone mass (Gratacós et al., 1999). As the disease progresses, ossification begins to ascend the vertebral column eventually fusing all of the vertebrae. The spine looses its flexibility (Ortner and Putschar, 1981) and begins to take on a "bamboo" look (Kidd, 1954; Zorab, 1961; Ortner and Putschar, 1981). As the ligaments near the spinal column begin to ossify (Ortner and Putschar, 1981; Hunter, 1989), AS can become confused with DISH. However, unlike DISH cases, AS ossification can affect the apophyseal joints (Arriaza, 1991; Aufderheide and Rodríguez-Martín, 1998). Also, most of the ossification corresponds to the annulus fibrosus fiber rather than the anterior longitudinal ligament. Figure 4 is an example of AS.

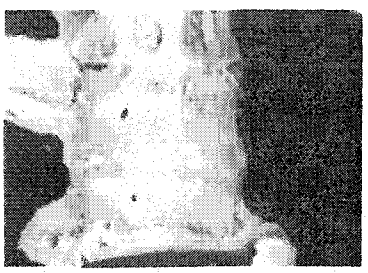

Fig. 4. Smithsonian Institution, Terry Collection #1635: Female, white, age 81: Ankylosing spondylitis.

Further, unlike DISH, ankylosing spondylitis can affect the costovertebral joints by fusing the ribs to the vertebrae (Arriaza, 1991; Aufderheide and Rodríguez-Martín, 1998). There is disagreement over

the exact sex ratio of AS, but the currently accepted range is from 2.5:1 to 5:1 male to female (Hoyle et al., 2000).

When distinguishing between AS and DISH it is useful to look at the formation of the ossification on the spine. In AS, the ossification of the anterior longitudinal ligament (ALL) is minor and tends to be symmetrical (Klepinger, 1970) whereas in DISH the ossification of the ALL is pronounced and tends to be right sided (Aufderheide and Rodríguez-Martín, 1998; Fairgrieve, 1999). Further, ossification in AS tends to be smooth (Ortner, 1987); in DISH anterior longitudinal ligament ossification is wavy or flowing (Forestier and Rotes-Querol, 1950). In AS there is vertebral squaring (Bourke, 1967; McEwan et al., 1971), which does not occur in DISH (Arriaza, 1993). Finally, DISH typically affects fewer vertebrae than AS, and the syndesmophytes in DISH form horizontally unlike the syndesmophytes in AS (Aufderheide and Rodriguez-Martín, 1998).

Another distinguishing factor between DISH and AS is the age of onset. The age of onset for AS is typically 16 to 30 years, but AS has been found in a child as young as 11 (François et al., 2000). Diffuse idiopathic skeletal hyperostosis, however, does not occur until at least 40 years of age (Arriaza, 1993).

Finally, it is important to look for the presence and condition of sacroilitis. While sacroilitis (SI) can occur in DISH, it is the hallmark of AS (Van der Linden et al., 1984; Rogers et al., 1985; Utsinger, 1985). To

distinguish between the SI caused by AS and DISH, it is important to look for erosions because they would indicate AS over DISH (Utsinger, 1985). Figure 5 shows erosions of the sacroiliac joint.

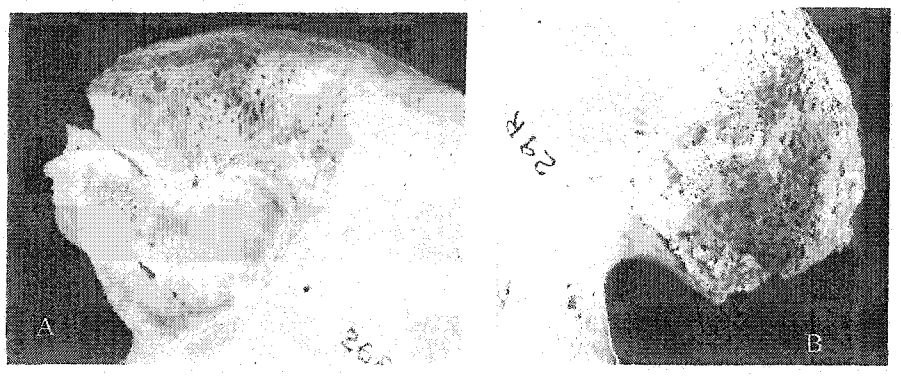

Fig. 5. **a:** Smithsonian Institution, Terry Collection #268: Male, White, age 62: Erosions of the SI joint. **b:** Smithsonian Institution, Terry Collection #29R: Female, white, age 84: Erosions of the SI joint.

In addition to the need to differentiate between ankylosing spondylitis and diffuse idiopathic skeletal hyperostosis, it is also important to realize that AS and DISH can coexist on the same spine. Figure 6 is an example an individual with ankylosing spondylitis and DISH. Thoracic vertebrae one through eight and 11 through 12 are fused by DISH ossification. Thoracic vertebrae nine through ten are fused by AS ossification.

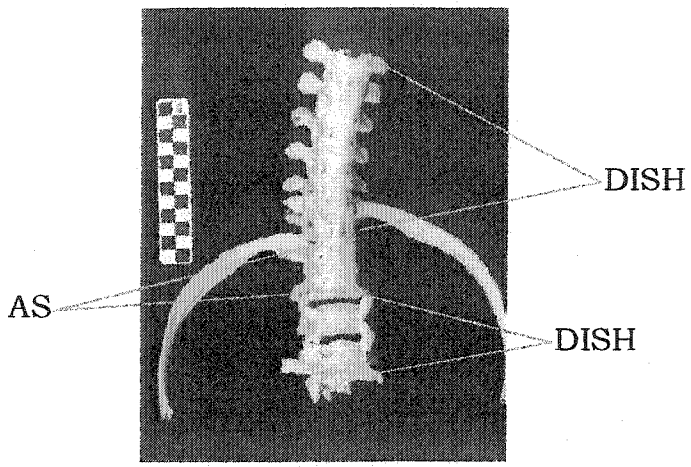

Fig. 6. Smithsonian Institution, Terry Collection #1635: Female, white, age 81: Example of AS and DISH on the same spine. Note the fusion of the ribs to the vertebrae, a condition typical of AS.

Reiter's syndrome. Reiter's syndrome (RS) is another of the seronegative spondyloarthropathies that could be confused with DISH. The disease primarily affects the feet, calcaneum, ankle and knee; however, there is spinal involvement associated with the condition as well (Rogers et al., 1987). When in the spine, Reiter's syndrome affects the thoracic and lumbar vertebrae (Arriaza, 1993). However, unlike DISH, the ossification in Reiter's syndrome does not always affect contiguous vertebrae; instead the ossification can "skip" vertebrae (Rogers et al, 1987). In addition to "skipping" vertebrae, RS can also affect the apophyseal joints, joints that are unaffected by DISH (Aufderheide and Rodríguez-Martín, 1998).

When diagnosing an individual with Reiter's syndrome, it is important to look at the entire skeleton. For instance, RS can have sacrolitic involvement but it is usually asymmetrical. Also, entheses may experience bone erosion as well as reactive new bone formation (Wilkens et al., 1981; Rogers et al., 1987; Cush and Lipsky, 1997).

Finally, when distinguishing between RS and DISH, it is of interest to note that the age of onset for Reiter's syndrome is 15 to 35 as opposed to the much later age of onset for DISH (Arriaza, 1993). While one would not make a diagnosis based on age alone, it would be exceedingly unlikely to encounter a 15 year old with DISH. Figure 7 shows a possible case of Reiter's syndrome.

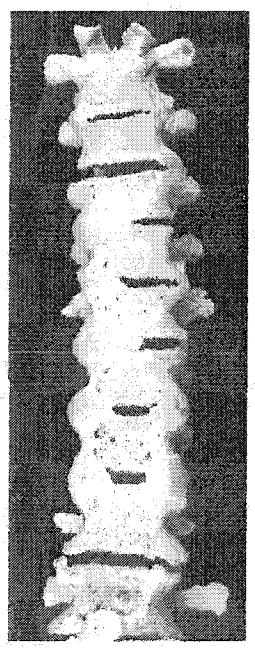

Fig. 7. Smithsonian Institution, Terry Collection #545: Male, white, age 44: Possible case of Reiter's Syndrome.

This individual died of coronary disease and exhibited signs of RS throughout the axial skeleton.

Psoriatic arthritis. Psoriatic arthritis (PA) is a seronegative spondyloarthropathy of unknown etiology that affects males and females equally (Bennett, 1997; Aufderheide and Rodriguez-Martín, 1998). Psoriatic arthritis usually strikes people when they are in their twenties or thirties; however, there is a childhood variety of PA that can occur when the child is 9 to 12 years old (Bennett, 1997).

Spinal manifestations of psoriatic arthritis look much like those of Reiter's syndrome. In both conditions there can be thick asymmetric ossification as well as "skipped" areas in the ossification formation (Zias and Mitchell, 1996).

The condition often affects the hands by destroying the phalanges and deforming the bones into a "cup-and-pencil" shape (Roger et al, 1987). Psoriatic arthritis also causes enthesopathies and erosive lesions primarily in the upper and lower limbs. Additionally, PA often unilaterally affects the sacroiliac joint (Zias and Mitchell, 1996).

Summary of spinal differential diagnosis. When attempting to diagnose a condition in an individual exhibiting spinal ossification, it is important to remember that there are multiple diseases that cause abnormal ossification. In order to differentiate DISH from RS and/or PA it is

essential to look at the entire skeleton, particularly the apophyseal joints and the hands and feet. If these areas are normal, then a diagnosis of DISH is likely. Also, when researching various diseases in an effort to make the most accurate diagnosis possible, it is important to remember that numerous names have been given to the same condition. In an attempt to alleviate some of the confusion Table 2 summarizes the differential diagnosis of DISH in conjunction with the diseases discussed in this section. Tables 3 and 4 summarize the various names given to all of the diseases discussed in this section.

TABLE 2. Differential diagnosis of DISH

	DISH	SD	AS	RS	PA
Vertebral Ossification	Yes	Yes	Yes	Yes	Yes
Type	Flowing	Flowing	Smooth	"Skip"	"Skip"
Apophyseal Ankylosis	No	No	Yes	Yes	Yes
Sacroilitis	Yes	No	Yes	Yes	Yes
Location	Both	----	Symmetric	Asymmetric	Asymmetric
Type	Non-erosive	----	Erosive	Both	Both
Age of Onset	40+	30+	20-30	15-35	20-30
Enthesopathies	Yes	No	Yes	Yes	Yes

TABLE 3. Summary of different names given to SD and AS

Spondylosis Deformans	Ankylosing Spondylitis
Degenerative Hypertrophic Spondylitis	Ankylopoietic Spondylitis
Degenerative Spondylosis	Bamboo Spine
Osteoarthritis	Bechterew's Disease
Osteophytosis	HLA-27 Spondyloarthropathy
Spondylitis Deformans	Marie-Strümple Disease
	Poker Spine
	Rheumatoid Spondylitis

TABLE 4. Summary of different names given to RS and PA

Reiter's Syndrome	Psoriatic Arthritis
Reactive Arthritis	

Extraspinal manifestations of DISH

Extraspinal manifestations of DISH come in the form of enthesopathies (Resnick et al., 1975; Utsinger, 1985; Crubézy, 1990), bony spurs that form in areas of tendon and ligament attachments (Benjamin et al., 2000). Enthesopathies can form either as a response to repetitive activity, as an inflammatory response to disease or as a product of aging (Niepel and Sit'aj, 1979; Dutour, 1986; Casas et al., 1996; Benjamin et al., 2000; Corthay et al., 2000).

Activity induced enthesopathies. Numerous reports have linked repetitive stressful activities to the production of enthesopathies and osseous changes in the skeleton (Merbs, 1983; Dutour, 1986; Sofaer Derevenski, 2000). For example, many sports require intense use of certain muscles and therefore can lead to injuries that result in bony spurs (Tyrdal, 1999). "Tennis elbow" is a classic example of how repetitive, stressful use of a muscle can lead to enthesopathies (Dutour, 1986). A subtler form of activity induced enthesopathies can be seen in the archaeological record. Based on enthesopathy patterns Hawkey and Merbs (1997) were able to conclude that Thule Eskimos from the northwest Hudson Bay made extensive use of kayaks in their subsistence efforts.

Activity induced enthesopathies are thought by some to be caused by micro-tears at muscle or ligament insertion points that in turn cause increased production of fibroblasts (connective tissue [Corthay et al., 2000]) and eventually ossification (Benjamin, 2000). Hawkey and Merbs (1995) state that enthesopathies are caused by increased capillary action in the periosteum due to repeated muscular/tendon stress, which in turn produces increased osteon remodeling resulting in enthesopathies.

Another theory proposed by Smith et al. (1994) postulates that enthesopathies are caused by micro fractures in trabecular bone. They believe that enthesopathies are formed to reinforce areas of the bone weakened by micro-cracks. However, a new study by Benjamin et al.

(2000) shows that enthesopathies can be formed by ossification within the fibrocartilage of muscle or ligament insertion, one of three cartilage types found in the human body (Anderson et al., 1998). Because the ossification occurs as part of normal growth, Benjamin et al. (2000) argue neither trauma nor inflammation need be present for the formation of bony spurs.

Disease and age induced enthesopathies. Just as in activity induced bony spurs, there have been numerous reports crediting DISH and other ossifying diseases with enthesopathy production (Utsinger, 1985; Beyeler et al., 1990; Curbézy, 1990; Corthay et al., 2000). However, despite making the association between the diseases and enthesopathy production, the reports do not give the actual mechanics of spur formation. A review of the literature shows that the events taking place at a cellular level during non-activity induced spur formation are not clearly understood (Corthay et al., 2000).

Areas of the skeleton most susceptible to enthesopathies. The need to distinguish between activity induced enthesopathies and inflammatory enthesopathies is somewhat circumvented in this research because it is assumed that if the individual has spinal DISH then the extraspinal enthesopathies are also likely due to DISH. However, to further ensure DISH enthesopathies alone are being recorded, tests of bilaterality were

run (see Chapter Three). Regardless of whether the enthesopathy is activity induced or the result of disease, it is still a product of aging. Enthesopathies have been found in young adults, but it is quite rare. Peak enthesopathy production occurs around age 60 in both males and females in all areas of the skeleton (Benjamin et al., 2000).

While enthesopathies can occur virtually anywhere muscles or ligaments attach to bone, there are areas that have a higher occurrence of DISH related enthesopathies. As expected, there is disagreement over which areas of the extraspinal skeleton DISH most effects. As a result, after reviewing the literature, this author selected and tested the main areas of the skeleton that most of the major researchers of DISH agree on. Those areas are: the scapula, proximal humerus, distal humerus, proximal ulna, proximal radius, iliac crest, proximal femur, anterior patella, proximal tibia, and the calcaneus (Forestier and Rotes-Querol, 1950; Resnick et al., 1975; Resnick and Niwayama, 1983; Resnick, 1985; Utsinger, 1985; Rogers et al., 1987; Crubézy, 1990; Arriaza, 1993; Suzuki et al., 1993; Aufderheide and Rodríguez-Martín, 1998; Benjamin et al., 2000).

Enthesopathies of the scapula. Areas of the scapula that are commonly affected by enthesopathies include the acromion (Crubézy, 1990) and just below the glenoid fossa (Resnick et al., 1975; Mann and Murphy, 1990). The acromion is one of two superior extensions of the scapula

and is located on the lateral side. The muscles that attach to the acromion, and therefore are susceptible to enthesopathy formation, are the deltoideus muscle and the trapezius muscle (White, 1991). The muscle that attaches below the glenoid fossa is the triceps muscle (Mann and Murphy, 1990).

The deltoideus is a large triangular shaped muscle with three points of origin: the anterior lateral third of the clavicle, the lateral margin and superior acromion, and the posterior end of the spine of the scapula. The three insertions eventually unite and form the deltoid tendon, which inserts into the deltoid prominence of the humerus. The muscle acting as a whole, serves to abduct the arm (Gray, 1956).

The trapezius muscle is also a triangular-shaped muscle with multiple points of origin: the external occipital protuberance, the spinous process of the seventh cervical vertebra, and the spinous processes of all thoracic vertebrae. From these origins the superior portion of the muscle inserts into the clavicle, the middle portion into the medial margin of the acromion, and part of the scapular spine. The inferior portion inserts into a tubercle near the scapular spine. When the muscle acts as a whole, it rotates the scapula (Gray, 1959).

The triceps brachii is a complex muscle consisting of three "heads" or separate, independent points of origin; those heads are the long head, lateral head, and medial head (Gray, 1959). For the purpose of this discussion, only the long head is of interest because it originates below

the glenoid fossa, specifically at the infraglenoid tubercle (Gray, 1959; White, 1991). From its point of origin, the long head eventually comes together with the other two heads to form the triceps tendon, which inserts into the olecranon of the ulna. Working as a whole, the triceps serves to extend the forearm, while the long head alone extends and adducts the arm (Gray, 1959). Figure 8 shows enthesopathies of the acromion and the infraglenoid tubericle.

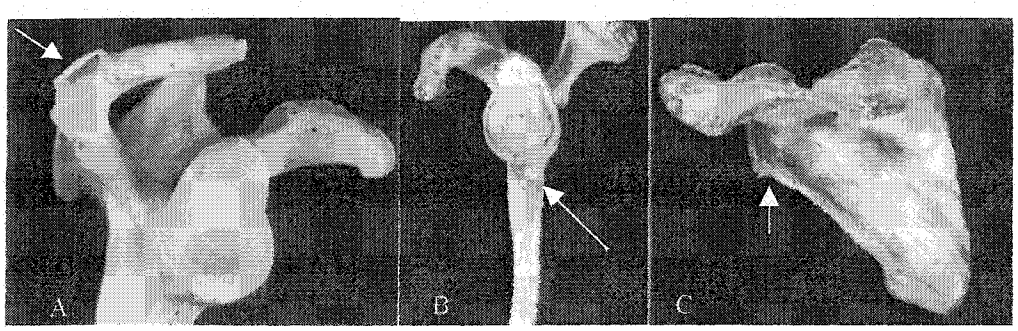

Fig. 8. **a:** Smithsonian Institution, Terry Collection #1258R: Female, black, age 50: Acromion enthesopathies. **b:** Smithsonian Institution, Terry Collection #775: Female, black, age 101: Infraglenoid fossa enthesopathies. **c:** Smithsonian Institution, Terry Collection #1292: Female, black, age 65: Infraglenoid fossa enthesopathies.

Enthesopathies of the proximal humerus. Areas of the proximal humerus that are typically affected by enthesopathies are the intertubercular sulcus or bicipital groove (Crubézy, 1990) and the deltoid

tubercle or deltoid prominence (Rogers, 1985). As its name implies, the bicipital groove houses the biceps brachii muscle and is thus susceptible to enthesopathies. The deltoid tubercle is the insertion point of the deltoid muscle (Gray, 1959), the muscle originating from the acromion whose function and anatomy were described in the preceding section.

The biceps brachii muscle is a fusiform muscle (Gray, 1959), meaning that it is tapered at both ends (Anderson et al., 1998). The muscle has two heads: a short head and a long head. The short head originates at the coracoid process of the scapula, and the long head originates at the supraglenoid tuberosity. The long head attaches to the humerus at the bicipital groove and eventually joins with the short head, inserting at the radial tuberosity as one tendon (Gray, 1959; White, 1991). When working as a whole, the biceps brachii serves to flex the forearm and supinate, or upturn, the hands. The long head by itself serves to reinforce the shoulder joint by pulling the humerus to the glenoid fossa (Gray, 1959). Figure 9 shows enthesopathies at the bicipital groove and the deltoid tubercle.

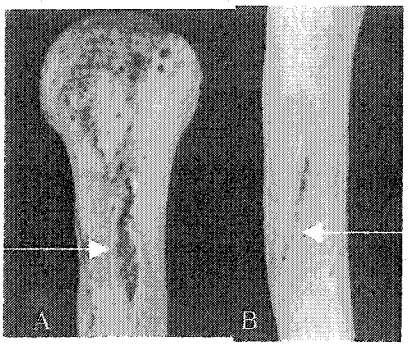

Fig. 9. Smithsonian Institution, Terry Collection #375: Male, black, age 59: **a:** Enthesopathies of the bicipital groove.

b: Enthesopathies of the deltoid tuberosity.

Enthesopathies of the distal humerus. The distal medial epicondyle is the area of the distal humerus that is prone to enthesopathies (Resnick et al., 1975) due to the attachment of the pronator teres muscle (Mann and Murphy, 1990). The pronator teres has two heads: the humeral head and the ulnar head. The humeral head originates at the medial epicondyle of the humerus while the ulnar head originates at the medial side of the coronoid process. The two heads intersect forming a tendon, which inserts on the lateral surface of the radius (Gray, 1959). Figure 10 shows enthesopathies of the humeral medial epicondyle.

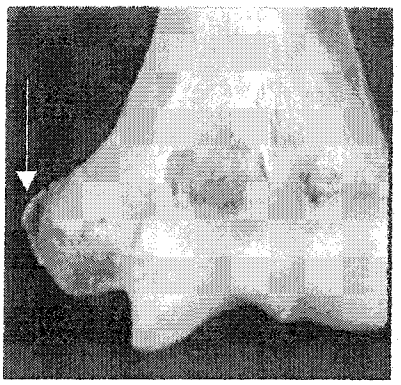

Fig. 10. Smithsonian Institution, Terry Collection #1231: Female, black, age 83: Medial epicondyle enthesopathy.

Enthesopathies of the proximal ulna. Enthesopathies of the proximal ulna typically occur at the ulnar olecranon (Resnick et al., 1975; Resnick, 1985; Utsinger, 1985; Crubézy, 1990). The olecranon process is the insertion site of the triceps brachii tendon (Gray, 1959; Mann and Murphy, 1990; White, 1991) and can experience extensive enthesopathy growth. The triceps brachii has three heads and originates in the shoulder area. Because of its point of origin, the triceps brachii has been discussed in detail in the "Enthesopathies of the Scapula" section of this chapter. Figure 11 shows one ulna with widespread enthesopathies of the olecranon process.

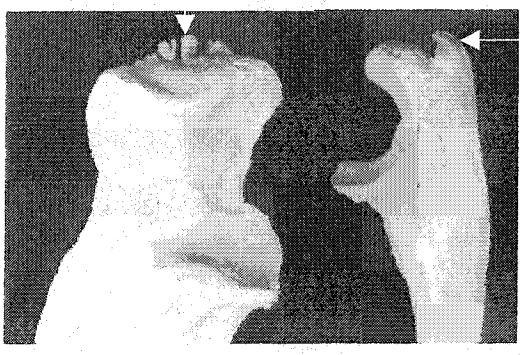

Fig. 11. Smithsonian Institution, Terry Collection #1214: Male, black, age 50: Enthesopathies of the olecranon process.

Enthesopathies of the proximal radius. The proximal radius is particularly enthesopathy prone in the area of the radial tuberosity (Rogers et al., 1987). The tuberosity is the insertion point of the biceps brachii, a two-headed muscle that originates in the shoulder area (Gray, 1959; Hall-Craggs, 1990; Mann and Murphy, 1990). Because of its origination point in the shoulder, the function and form of the biceps brachii has been detailed in the "Enthesopathies of the Proximal Humerus" section of this chapter. Figure 12 shows enthesopathy formation in the radial tuberosity. The radius on the left, Terry #1214, has extensive enthesopathy formation in and around the tuberosity. The radius on the right, Terry #1202R, has no enthesopathy development and is shown for the sake of comparison. It is interesting to note how the enthesopathy formation curves with the arc of the tuberosity.

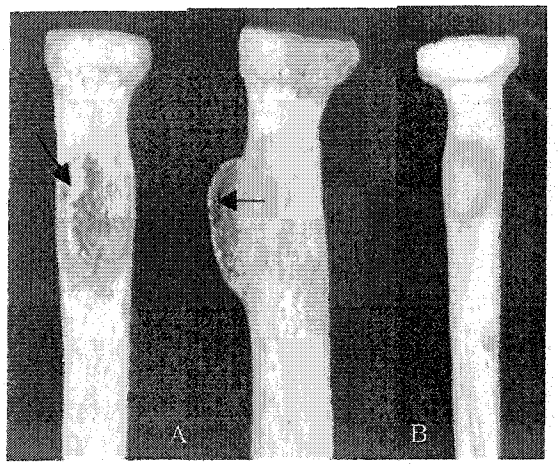

Fig. 12. **a:** Smithsonian Institution, Terry Collection #1261: Male, black, age 60: Radial tubercle enthesopathies. **b:** Smithsonian Institution, Terry Collection #1202R: Female, white, age 56: No enthesopathies.

Enthesopathies of the iliac crest. When a person is affected by DISH, the iliac crest is likely to experience enthesopathic ossification (Forestier and Rotes-Querol, 1950; Resnick et al., 1975; Resnick, 1985; Rogers et al., 1985; Crubézy, 1990; Aufderheide and Rodríguez-Martín, 1998). The entire crest is prone to enthesopathies because numerous abdominal muscles originate on the crest. Because multiple muscles originate on the iliac crest, it is easier to divide the crest into three sections as did Gray (1959) when discussing the various muscles. Gray divided the crest into an external lip, internal lip, and an intermediate line. Each section is the point of origin for multiple muscles. The external lip houses the tensor fasciae latae, obliquus externus abdominis, latissimus

dorsi, and the fascia lata. The intermediate line houses the obliquus internus abdominis. The internal lip is the point of origin for the fascia iliaca, transversus abdominis, quadratus lumborum, sacrospinalis and the iliacus. Many of these muscles insert in the vertebral column or ribs. Some abdominal muscles play a role in the function of the diaphragm (Gray, 1959). Figure 13 shows extensive ossification on the iliac crest due to diffuse idiopathic skeletal hyperostosis. It is interesting to note how the ossification follows the arc of the iliac crest.

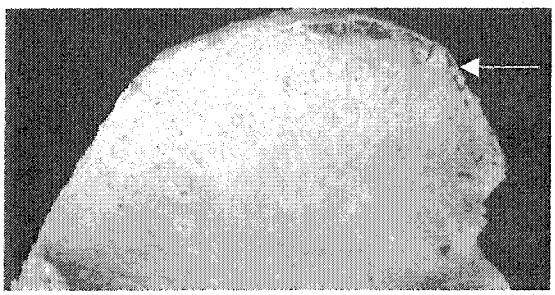

Fig. 13. Smithsonian Institution, Terry Collection #1261: Male, black, age 60: Enthesopathy formation on the iliac crest.

Enthesopathies of the proximal femur. Areas of the proximal femur that are vulnerable to enthesopathies include the greater and lesser trochanters, the trochanteric fossa, and the linea aspera (Resnick and Niwayama, 1983; Rogers et al., 1987; Mann and Murphy, 1990; Aufderheide and Rodríguez-Martín, 1998). The anterior portion of the greater trochanter is the insertion site of the gluteus minimus, while the posterior portion is the insertion point of the gluteus medius. The lesser

trochanter is the insertion point for the iliopsoas tendon, which has two parts, the iliacus muscle and the psoas major muscle (Gray, 1959). The trochanteric fossa is the insertion site for the obturator externus tendon. Finally, the linea aspera is the origin site of the vastus muscles and the insertion site of the longis, brevis, and magnus muscles, collectively known as the adductors (Gray, 1959; White, 1991).

The greater trochanter is the insertion site of both the gluteus medius and gluteus minimus, which have their origins in the pelvic area. They are responsible for abducting and rotating the thigh medially and laterally (Gray, 1959).

One of the two parts of the iliopsoas muscle, the psoas major, is a fusiform muscle originating from the lumbar vertebrae and inserting into the lesser trochanter of the femur. It allows the thigh to flex and rotate medially, and allows the lumbar vertebrae to flex and to bend laterally. The second part of the iliopsoas muscle, the iliacus, originates at the ilium and also inserts in the lesser trochanter. It is responsible for flexion and medial rotation of the thigh (Gray, 1959).

The obturator externus is a triangular muscle that originates near the obturator foramen and inserts in the trochanteric fossa of the femur. The function of the obturator externus is to laterally rotate the thigh (Gray, 1959).

The linea aspera is the point of origin for the vastus muscles, which are comprised of the vastus lateralis, vastus medialis and vastus

intermedius. All of these muscles eventually come together to form three-fourths of the quadriceps femoris tendon, which inserts in the patella. The three vastus muscles, when working together as a part of the quadriceps tendon, extend the leg (Gray, 1959).

The adductor muscles insert in the linea aspera. Each of the three adductors originates around the pubic/ischial area and plays a key role in adducting the thigh. They also allow the thigh to flex and to rotate medially and laterally (Gray, 1959). Figure 14 shows enthesopathies of the greater and lesser trochanters, the trochanteric fossa, and the linea aspera.

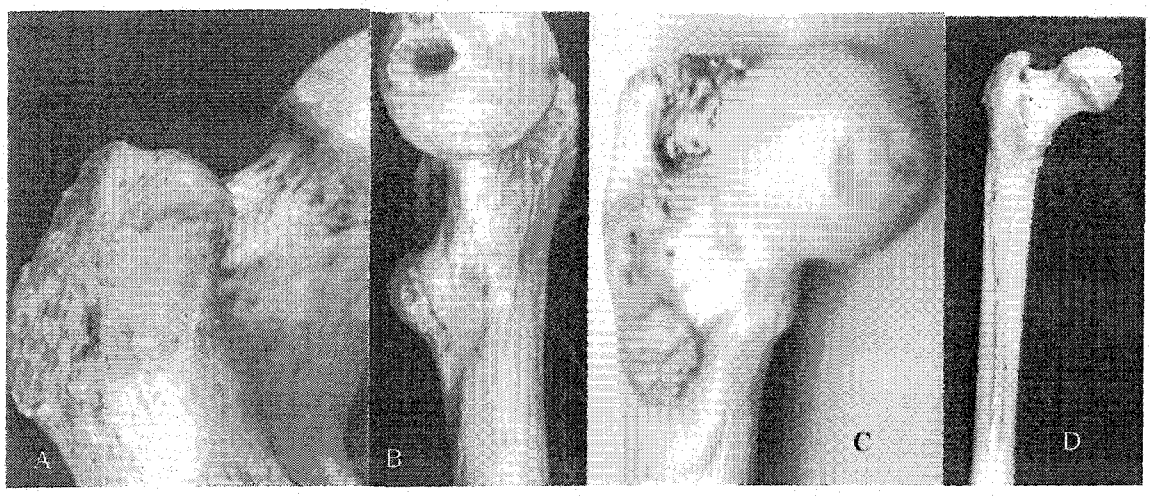

Fig. 14. **a:** Smithsonian Institution, Terry Collection #375: Male, black, age 59: Enthesopathies on the greater trochanter. **b:** Smithsonian Institution, Terry Collection #775: Female, black, age 101: Lesser trochanter. **c:** Smithsonian Institution, Terry Collection #375: Male, black, age 59: Trochanteric fossa. **d:** Smithsonian Institution, Terry Collection #1231: Female, black, age 83: Linea aspera.

Enthesopathies of the patella. Other areas susceptible to DISH enthesopathies are the anterior and superior surfaces of the patella (Resnick et al., 1975; Resnick, 1985; Resnick and Niwayama, 1985; Utsinger, 1985; Rogers et al, 1987; Crubézy, 1990; Crubézy and Trinkaus, 1992; Aufderheide and Rodríguez-Martín, 1998). The patella is vulnerable to enthesopathies due to the insertion of the quadriceps femoris tendon (Rogers et al., 1987; White, 1991; Crubézy and Trinkaus, 1992). The quadriceps femoris tendon, which was mentioned in the discussion of the linea aspera, is comprised of four muscles: the rectus

femoris, the vastus lateralis, the vastus medialis, and the vastus intermedius (Gray, 1959).

The rectus femoris is a fusiform muscle with two separate points of origin. The first point is along the iliac spine while the second point originates near the acetabulum. The two areas of the muscle eventually unite becoming a tendon, and insert into the base of the patella. By itself the rectus femoris allows the thigh to flex. When used as a part of the entire quadriceps tendon, the rectus femoris gives even more movement (Gray, 1959).

The vastus lateralis is a large muscle that originates from an aponeurosis (Gray, 1959), a large sheet of strong fibers that act like a tendon in order to attach the muscle to bone (Anderson et al., 1998). The aponeurosis has multiple points of origin, one of which is the linea aspera. The vastus lateralis is the largest part of the quadriceps femoris and mingles with many other muscles on its way to its insertion point on the patella (Gray, 1959).

The vastus medialis also has multiple points of origin and mingles with various muscles, such as the adductor longus and the adductor magnus, on its way to the patella. Fibers from the vastus medialis become part of an aponeurosis (Gray, 1959), which, in addition to binding muscle to bone, can bind muscles to each other (Anderson et al., 1998). The muscle eventually inserts into the medial border of the

patella where it joins with the rest of the quadriceps femoris (Gray, 1959).

The final part of the quadriceps tendon is the vastus intermedius, which originates from various points along the femur. The muscle forms into an aponeurosis near its insertion point on the patella, allowing the muscle to reinforce the quadriceps. The quadriceps femoris tendon as a whole allows the entire leg to extend (Gray, 1959). Figure 15 shows the enthesopathic ossification of the quadriceps tendon on the patella.

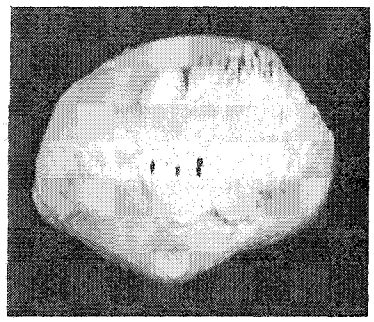

Fig. 15. Smithsonian Institution, Terry Collection #1214: Male, black, age 50: Enthesopathy of the patella.

Enthesopathies of the proximal tibia. The tibia has two main areas that are the most susceptible to enthesopathies: the tibial spines and the soleal line (Utsinger, 1985; Mann and Murphy, 1990). The tibial spines, or the medial and lateral intercondylar tubercles, are the insertion points for the anterior and posterior cruciate ligaments and the anterior and

posterior portions of the menisci ligament. The soleal, or popliteal, line is the insertion point for the popliteus muscle (White, 1991).

The cruciate ligaments get their name in part because they cross each other as they traverse the area between their origin and insertion points. They are very strong ligaments and are located in the knee joint. The menisci ligaments are also in the knee joint. They are located on the head of the tibia and articulate with the femoral condyles. The menisci are surrounded by a synovial membrane and deepen the area of the medial and lateral tibial condyles. The result is a stronger, smoother articulation with the femur (Gray, 1959).

The popliteus muscle is a flat triangular muscle that originates on the lateral condyle of the femur. It inserts near the upper portion of the soleal line of the tibia. The popliteus muscle works to flex the leg and to medially rotate the leg (Gray, 1959). Figure 16 shows enthesopathies of the tibial spines and the soleal line.

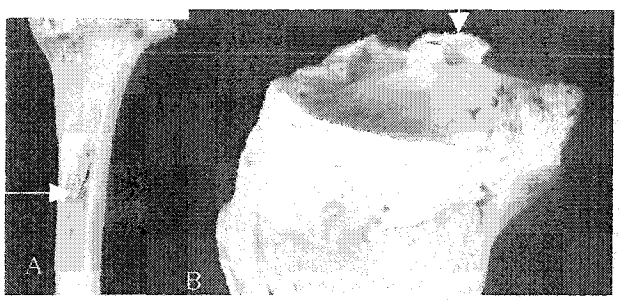

Fig. 16. Smithsonian Institution, Terry Collection #375: Male, black, age 59: **a:** Soleal line enthesopathies. **b:** Tibial spine enthesopathies.

Enthesopathies of the calcaneus. Enthesopathies are quite common on the calcaneus and are usually located in the posterior and inferior sections of the bone (Resnick et al., 1975; Resnick and Niwayama, 1983; Resnick, 1985; Mann and Murphy, 1990; Benjamin et al., 2000). The calcaneus is the largest of the foot bones and is the insertion point of the strongest tendon in the human body, the Achilles tendon (Resnick et al., 1977; White, 1991). While the Achilles tendon inserts in the posterior area, the plantaris inserts into the posterior inferior section of the calcaneus (Gray, 1959).

The Achilles tendon is actually part of a larger muscle known as the gastrocnemius. The gastrocnemius originates in the fibula and makes up most of the calf muscle. As the gastrocnemius nears its insertion point, it forms an aponeurosis from which it joins with the soleus. The two muscles then become the Achilles tendon (Gray, 1959).

The plantaris originates from the linea aspera and the popliteal ligament of the knee joint. It is situated between the gastrocnemius and soleus and eventually inserts in the inferior posterior calcaneus (Gray, 1959). Figure 17 shows enthesopathies of the Achilles tendon and the plantaris.

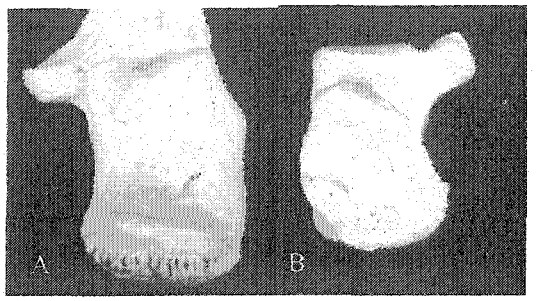

Fig. 17. **a:** Smithsonian Institution, Terry Collection #1214: Male, black, age 50: Achilles tendon enthesopathies. **b:** Smithsonian Institution, Terry Collection #1202R: Female, white, age 56: Achilles tendon enthesopathies.

Differential diagnosis of extraspinal conditions

Just as with spinal ossification, there are multiple diseases that cause osseus growth or remodeling throughout the extraspinal skeleton. Some of those conditions include degenerative joint disease, activity induced pathology, and the seronegative spondyloarthropathies (Shaibani et al., 1993).

Degenerative joint disease. Degenerative joint disease (DJD), also known as osteoarthritis (Rothschild et al., 1999), is a very common ailment throughout the animal kingdom having been found frequently in practically all mammals and most primates (DERousseau, 1985). In humans, degenerative joint disease is one of the most common skeletal pathologies found in archaeological populations dating from the time of Neanderthals to the present (Jurmain, 1977; Jurmain, 1990).

Osteoarthritis is generally thought to be a product of aging and extensive use of certain joints. Studies have shown that a general pattern of osteoarthritis can be discerned in archaeological populations and as a result can reveal something about the activities of the people suffering from it (Bridges, 1991). A study by Knüsel et al. (1997) questioned the ability of DJD to predict activities; however they focused only on spinal DJD whereas Bridges (1991) and others have focused on extraspinal DJD, which is more likely to reflect activity patterns.

Degenerative joint disease is characterized by bone remodeling, eburnation, small cysts, and narrowing of joint space (Aufderheide and Rodríguez-Martín, 1998). It can be distinguished from DISH caused enthesopathies by its location and the presence of eburnation and cysts. In DJD the entire joint can be affected whereas in DISH only areas of muscle or tendon insertion are involved. DJD shows some level of eburnation or a smooth polished bone surface; DISH enthesopathies do not. Figure 18 shows a case of osteoarthritis.

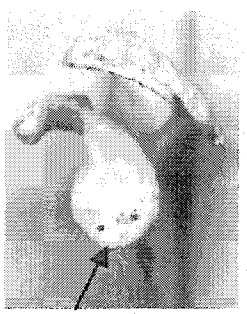

Fig. 18. Smithsonian Institution, Terry Collection #1134R: Female, black, age 71: Scapula exhibiting osteoarthritis or DJD.

Activity induced pathology. Activity induced enthesopathies were discussed in detail in a previous section of this chapter and thus will not be further explained here. However it bears pointing out that while repetitive activity can cause enthesopathies, for the purposes of this study if the enthesopathies are bilateral and the individual has spinal DISH then the enthesopathies are assumed to be a product of DISH.

Seronegative spondyloarthropathies. In addition to the spinal manifestations of the suite of seronegative spondyloarthropathies, SNS can also cause enthesopathies (Shiabani et al., 1993). However, as with activity induced enthesopathies, for the purposes of this study, if the individual has spinal DISH, does not have any of the spinal seronegative spondyloarthropathies, and the enthesopathies are bilateral, it is assumed that the observed enthesopathies are a product of DISH not SNS.

CHAPTER 3

MATERIALS AND METHODOLOGY

Materials

The population used for data collection in this study was the Terry Collection, housed at the Smithsonian Institution, National Museum of Natural History. The Terry Collection is an anatomical collection comprised of 1728 individuals who lived between 1822 and 1943. Dr. Robert J. Terry created the collection over many years by assembling cadavers of people who were either unclaimed indigents or who donated their bodies to science. Each individual has documentation giving various information such as biological affinity, sex, cause of death, and most importantly for this research, age at death. Because the individuals in the Terry Collection were contemporaneous to those building the collection, the information for each person is known and did not have to be inferred through anthropological techniques (Hunt, 2000).

The Terry Collection is made up of individuals from three distinct biological affinity groups. The Smithsonian Institution has labeled the groups "black," "white," and "Asian." For the sake of continuity, the author is using the Smithsonian's biological affinity terms.

Methodology

Because the point of this research is to create another method for estimating age at death, it is essential to gather data from a population in which age at death is known. If standard osteological aging methods were used to age the individuals, then the errors inherent in the various methodologies would be imbedded in the methodology this research is creating. As a result, the Terry Collection was ideal for this thesis. Table 5 summarizes the demography of the Terry Collection.

TABLE 5. Demography of the Terry Collection

	Males	Females	Unknown	Total
White	461	323	0	784
Black	546	392	0	938
Asian	5	0	0	5
Unknown	0	0	1	1
Total	1012	715	1	1728

How the data were gathered. There is some disagreement among researchers as to when a diagnosis of DISH can be made. According to some, there need be fusion of only two vertebrae (Mann and Murphy, 1990), other opinions state there must be anywhere from three to four consecutively fused vertebrae (Rogers et al., 1987; Aufderheide and Rodriguez-Martín, 1998). The author chose to follow a scoring system

created by Arriaza (2000) in order to test the replicability of the method and to use it as a springboard for creating the aging technique. The scoring system has five categories: absent, incipient, mild, moderate and severe. The categories are based solely on spinal manifestations and are defined in Table 6.

TABLE 6. Definitions of DISH categories

Degree	Definition
Absent	no DISH present
Incipient	extremely small spurs or hyperostosis in one or more vertebrae
Mild	clearly visible spurs, normally unfused in one or more vertebrae; at least one but no more than three vertebrae have severe spurs
Moderate	more than three vertebrae are affected with severe spurs or fusion at least three vertebrae
Severe	obvious large spurs with or without fusion in more than four vertebrae

Figure 19 illustrates each category of DISH.

When DISH was diagnosed in the spine, other parts of the skeleton were examined for enthesopathies. While enthesopathies can occur anywhere in the body, only the enthesopathies of very specific muscles were considered in this study. These areas of the skeleton were chosen after an exhaustive literature review of extraspinal DISH showed them as the places most researchers agreed as being prone to DISH (Resnick et al., 1975; Crubezy, 1990).

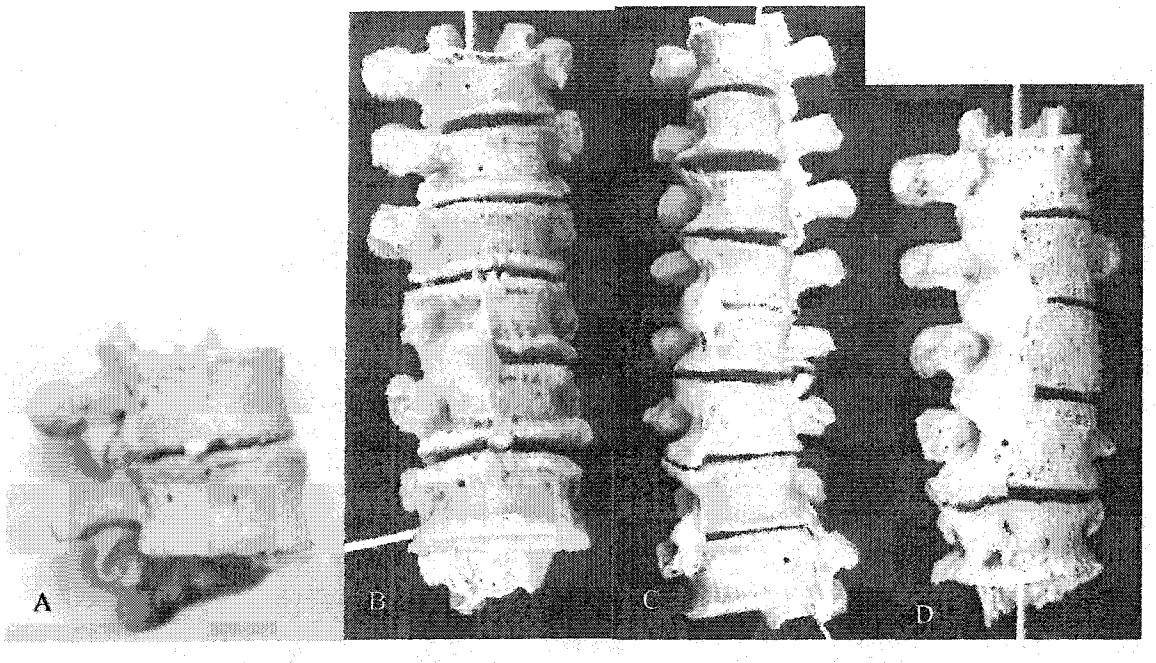

Fig. 19. **a:** Smithsonian Institution, Terry Collection #1269R: Female, black, age 69: Incipient DISH. **b:** Smithsonian Institution, Terry Collection #1134R: Female, black, age 71: Mild DISH. **c:** Smithsonian Institution, Terry Collection #1233R: Female, white, age 63: Moderate DISH. **d:** Smithsonian Institution, Terry Collection #781R: Female, white, age 70: Severe DISH.

Table 7 lists the enthesopathies measured in this study. As the measurements were taken they were recorded on data collection forms. For sample forms, see APPENDIX I.

TABLE 7. Extraspinal enthesopathy areas examined

Bone	Location	Side
Scapula	Acromion	Left, Right
Scapula	Infraglenoid Fossa	Left, Right
Humerus	Bicipital Groove	Left, Right
Humerus	Deltoid Tuberosity	Left, Right
Humerus	Medial Epicondyle	Left, Right
Ulna	Olecranon	Left, Right
Radius	Radial Tuberosity	Left, Right
Ilium	Iliac Crest	Left, Right
Femur	Greater Trochanter	Left, Right
Femur	Lesser Trochanter	Left, Right
Femur	Trochanteric Fossa	Left, Right
Femur	Linea Aspera	Left, Right
Patella	Anterior Patella	Left, Right
Tibia	Tibial Spines	Left, Right
Tibia	Soleal Line	Left, Right
Calcaneus	Posterior	Left, Right
Calcaneus	Inferior	Left, Right

Spinal analysis

The author diagnosed and scored the degree of DISH in each individual in the Terry Collection, taking care to note the individuals Arriaza previously analyzed in order to test the replicability of the scoring system. Once the individuals were categorized, the spinal ossification was measured in millimeters with sliding calipers. Three measurements were taken: length of the entire ossification segment (Fig. 20 A), maximum width (Fig. 20 B), and maximum ossification border thickness on the vertebral body (Fig. 20 C). If the ossification within one block was not fused then the length of each individual segment within the block was measured then added together to produce the maximum length of the ossification (Fig. 21). After recording each measurement, the ossification volume was calculated:

volume = maximum length x maximum width x maximum ossification border thickness on vertebral body

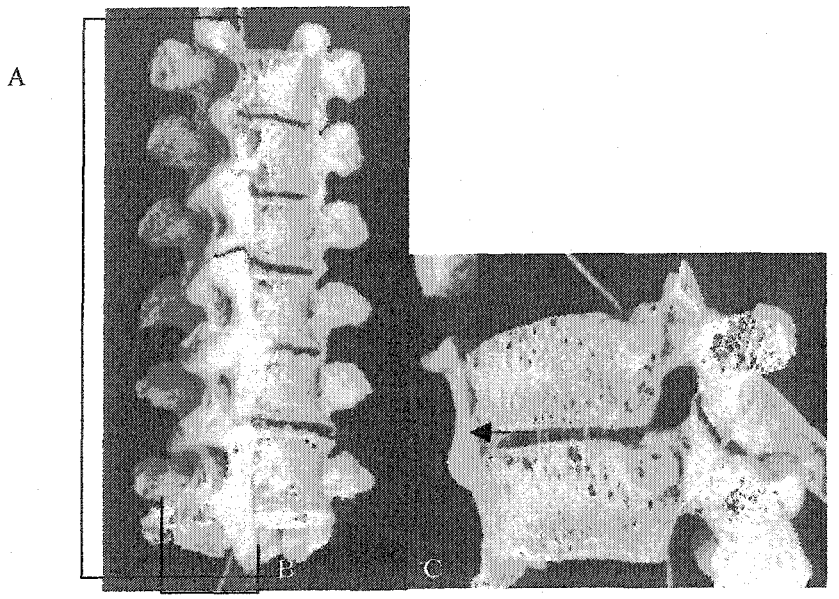

Fig. 20. **a:** Smithsonian Institution, Terry Collection #842: Male, white, age 73: Area of maximum length. **b:** Smithsonian Institution, Terry Collection #842: Male, white, age 73: Area of maximum width. **c:** Smithsonian Institution, Terry Collection #268: Male, white, age 62: Maximum ossification border thickness on the vertebral body.

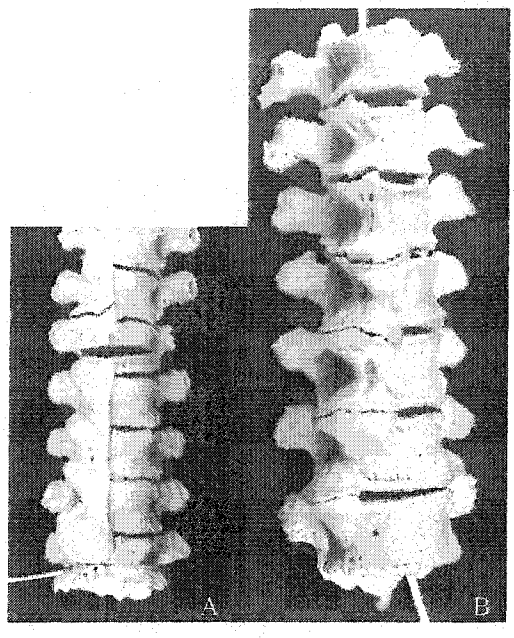

Fig. 21. **a:** Smithsonian Institution, Terry Collection #1069: Female, white, age 70: One block of broken ossification. **b:** Smithsonian Institution, Terry Collection #24R: Female, black age 52: Unfused vertebral ossification.

Statistical analysis of spinal ossification. Chi square tests were run to test for significant differences between sex and biological affinity within the DISH affected sample. Pearson product-moment correlation coefficient tests were performed to test the relationship between: 1) age versus DISH ossification volume while controlling for sex and biological affinity; 2) age versus individual DISH ossification measurements (maximum length, maximum width, and maximum ossification border thickness on the vertebral body) while controlling for sex and biological affinity; 3) age versus DISH ossification volume within each degree of

severity category while controlling for sex and biological affinity; 4) age versus individual DISH ossification measurements (maximum length, maximum width, and maximum ossification border thickness on the vertebral body) within each degree of severity category while controlling for sex and biological affinity. Finally, based on the correlations, regression equations were created for DISH affected individuals as a whole, controlling for sex, and for each degree of severity category. Unfortunately, when running the regression statistics, many DISH affected individuals had to be rejected from the sample due to having other severe spondyloarthropathies in addition to DISH, or due to postmortem ossification breakage. Due to the modified sample size, the incipient and mild categories had to be pooled as did the moderate and severe categories, while still controlling for sex.

Extraspinal analysis

When enthesopathies were present, three measurements were taken from the largest spur in each area: maximum height, maximum width, and maximum thickness. If enthesopathies were present on the left and right bones of the same element (i.e. the left and right femur) measurements were still taken for each bone – both left and right. After recording the measurements, volumes were calculated for each enthesopathy.

volume = maximum height x maximum width x maximum thickness

Most enthesopathic measurements are straightforward; however, measurements on the ulna, radius, iliac crest, patella, and calcaneus warrant some explanation.

Ulna. Enthesopathies on the proximal end of ulnae are found on the olecranon process (Mann and Murphy, 1990). Because it is difficult to tell where the enthesopathies begin when viewing them from the posterior side of the bone, a depth measurement should be taken from the anterior side. The width measurement should be taken from the posterior side of the spurs as a unit – not just the tip of an individual spur. Figure 22 illustrates how the spurs were measured.

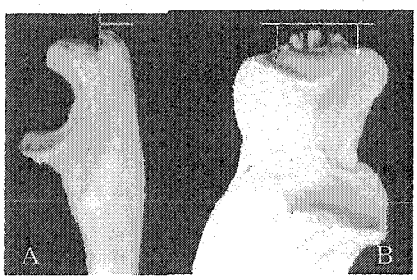

Fig. 22. **a:** Smithsonian Institution, Terry Collection #1214: Male, black, age 50: Depth measurement from anterior side of ulna – measures maximum enthesopathy height. **b:** Smithsonian Institution, Terry Collection #1214: Male, black, age 50: Width measurement of enthesopathy on ulna.

Radius. Enthesopathy formation on the proximal radius takes place in the radial tuberosity. When the spur arcs around the tuberosity, it should be measured with a flexible tape measure. The arc is considered the width, the height measurement is taken inside the tuberosity and the thickness is horizontal to longest plane of the radius. Figure 23 illustrates these measurements.

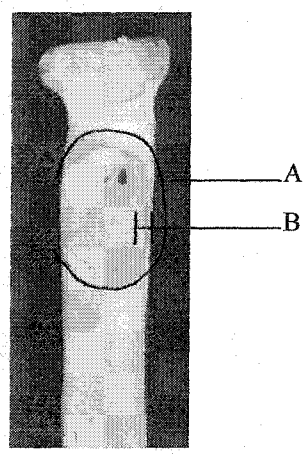

Fig. 23. Smithsonian Institution, Terry Collection #1214: Male, black, age 50: **a:** Width measurement. **b:** Thickness measurement.

Iliac crest. The iliac crest is another place where enthesopathies form. The width of the enthesopathies was measured using a tape measure to calculate the width of the arc. Using sliding calipers, the height was measured from the blade side of the spurs. Figure 24 illustrates the specific measurements.

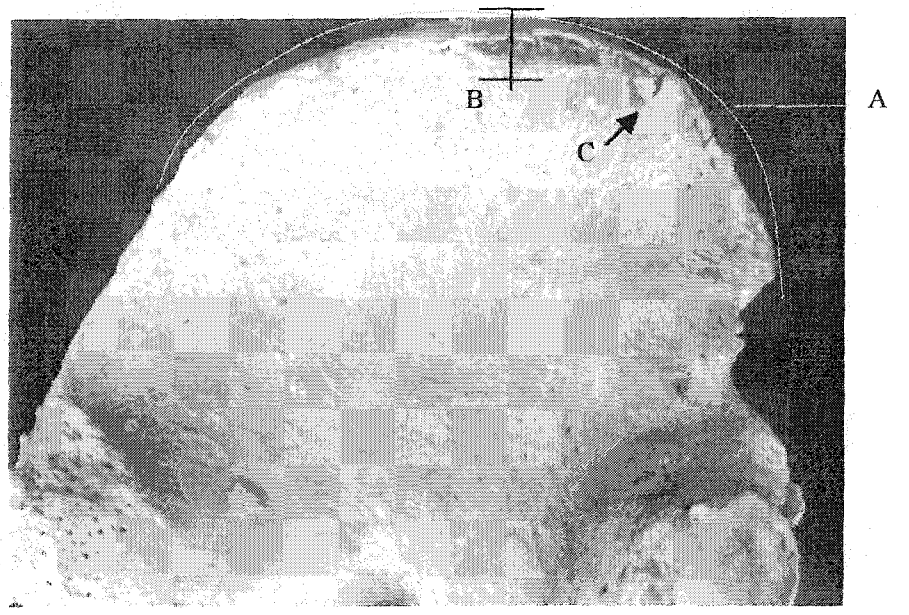

Fig. 24. Smithsonian Institution, Terry Collection #1261: Male, black, age 60: **a:** Width. **b:** Thickness. **c:** Height.

Patella. Enthesopathies often occur on the anterior side of the patella. Commonly, when enthesopathies are DISH related, they transverse the entire length of the anterior surface (Mann and Murphy, 1990). The maximum height, width and thickness of the enthesopathies were measured; the measurements are illustrated in Figure 25.

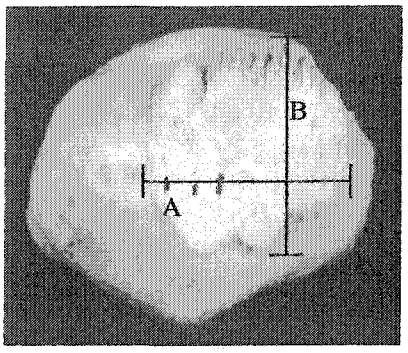

Fig. 25. Smithsonian Institution, Terry Collection #1214: Male, black, age 50: **a:** Width. **b:** Height.

Calcaneus. Commonly, enthesopathies are found superiorly and inferiorly on the calcaneus (Mann and Murphy, 1990). When measuring the height of the enthesopathies it is important to be consistent in where the measurement is taken. The height measurement was taken from the anterior side of the spur in this study. The anterior side was chosen because the beginning of the spur was obvious when viewed from this side. Determining where the spur began on the posterior side of the spur was somewhat subjective. Figure 26 illustrates this point and shows where the measurement should be taken.

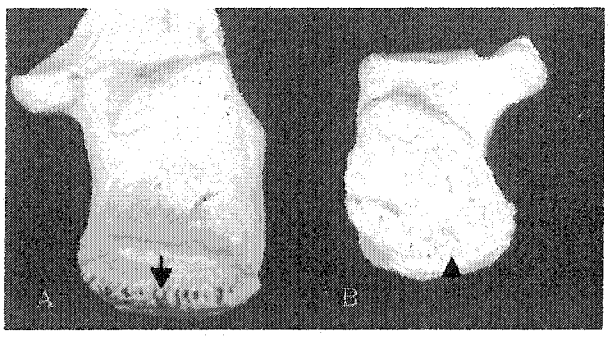

Fig. 26. **a:** Smithsonian Institution, Terry Collection #1214: Male, black, age 50: Area height measurement taken from.
b: Smithsonian Institution, Terry Collection #1202R: Female, white, age 56: Area of difficulty in assessing where the spur begins.

Statistical analysis of extraspinal ossification. As with the spinal analysis, Pearson product-moment correlation coefficient tests were performed to test the relationship between: 1) age versus extraspinal DISH ossification volumes while controlling for sex and biological affinity; and 2) age versus extraspinal DISH ossification volumes within each degree of severity category while controlling for sex and biological affinity. Also, to ensure that the extraspinal measurements used in the regression equations were truly DISH related instead of representations of handedness or other enthesopathy causing factors, extraspinal ossification was tested for bilaterality using Pearson's r.

Assumptions inherent in the methodology

The basic assumptions of the methodology are that 1) DISH is an age related condition that develops in a fairly uniform manner and thus it can be used to estimate biological age in an individual; 2) that the Terry Collection represents an appropriate cross-section of a relatively modern United States population.

CHAPTER 4

RESULTS

The Terry Collection is comprised of 1007 males and 715 females. Of those individuals, 70 males and 24 females have DISH representing 6.95% of males and 3.35% of females respectively. These values are significantly different ($X^2 = 12.12$; $p < 0.05$). However, there are no significant differences between black and white biological affinity categories ($X^2 = 4.67$; $p > 0.05$). Because there are only five Asians in the sample, this category was not included in the chi square test.

The DISH scoring methodology that was being tested as part of this thesis was successful. This author and the scoring system's creator (Arriaza, 2000) had a concordance rate of 97%. The author and Arriaza independently diagnosed and scored the level of DISH in 102 individuals from the Terry Collection. The final scoring system, which is based solely on the spinal manifestation of DISH, was defined in Chapter Three. Tables 8 and 9 and figures 27 and 28 show the breakdowns of degrees of DISH affected individuals based on sex and biological affinity categories.

TABLE 8. DISH by degree of severity and sex

Condition	Female	Male	Total
Incipient	4 (16%)	16 (23%)	20
Mild	4 (16%)	18 (26%)	22
Moderate	7 (29%)	19 (27%)	26
Severe	9 (38%)	17 (24%)	26
Total	24	70	94

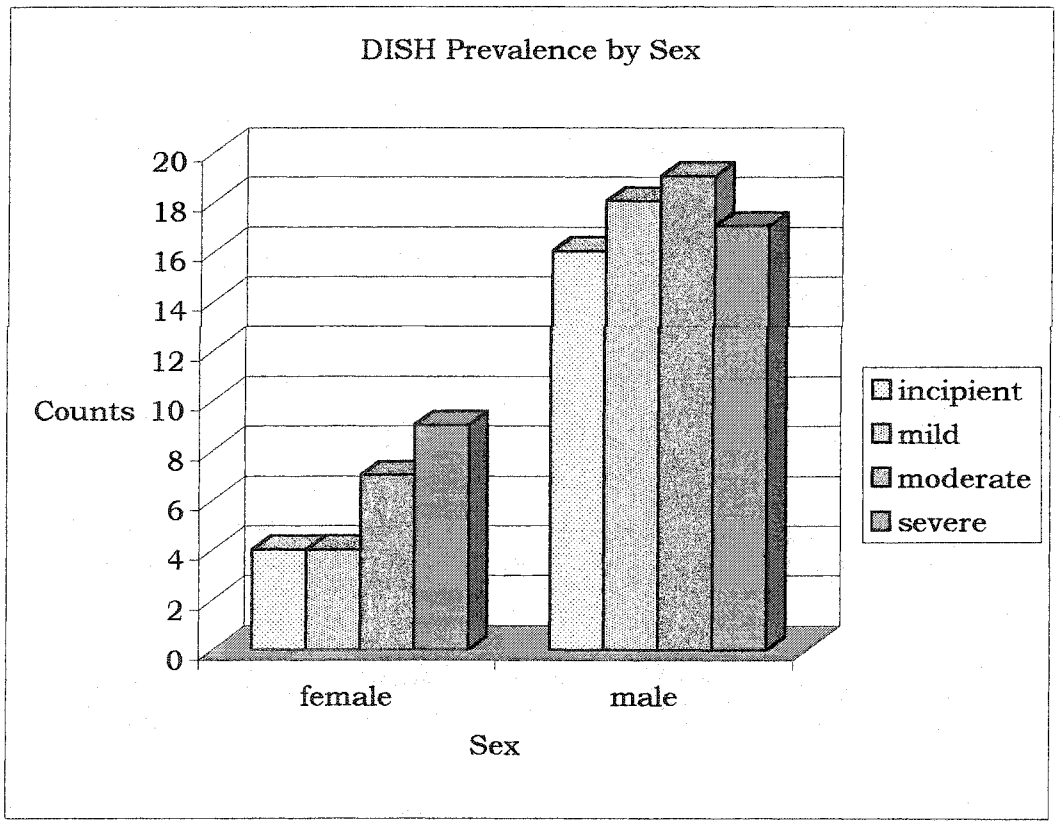

Fig. 27. DISH prevalence and degree of severity by sex.

TABLE 9. DISH by degree of severity and biological affinity

Condition	Asian	Black	White	Total
Incipient	1 (50%)	10 (22%)	9 (20%)	20
Mild	1 (50%)	13 (28%)	8 (17%)	22
Moderate	0 (0%)	14 (30%)	12 (26%)	26
Severe	0 (0%)	9 (20%)	17 (37%)	26
Total	2	46	46	94

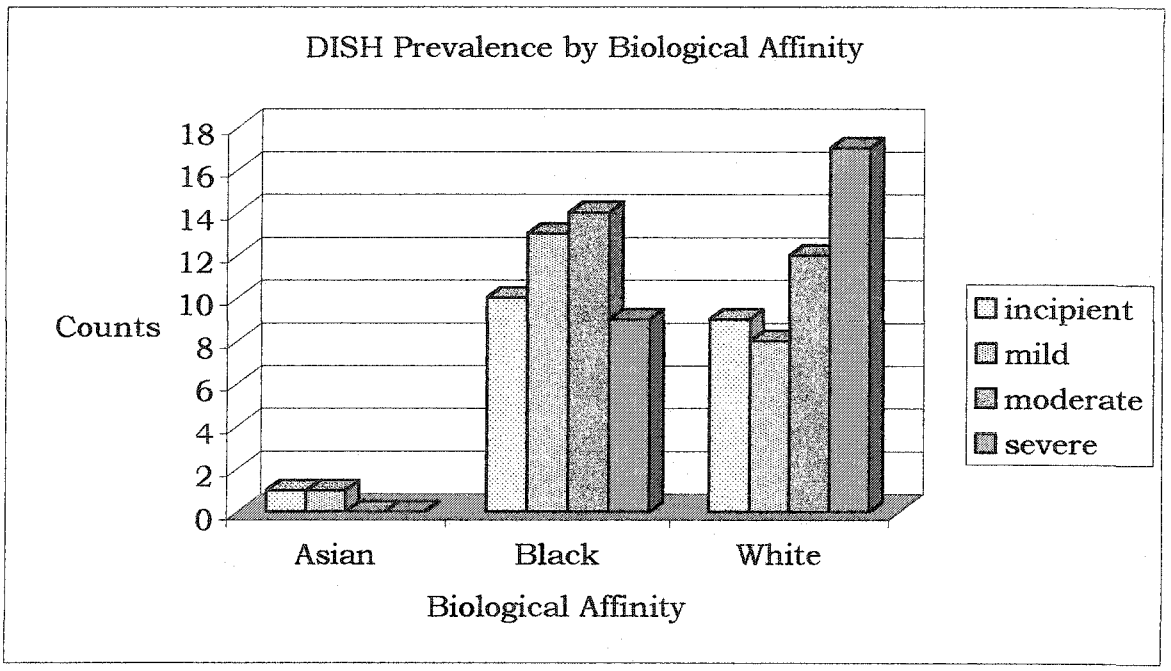

Fig. 28. DISH prevalence and degree of severity by biological affinity.

TABLE 10. DISH by degree of severity and sex within biological affinity categories

	Asian		White		Black		
	Male	Female	Male	Female	Male	Female	Total
Incipient	1	0	7	2	8	2	20
Mild	1	0	8	0	9	4	22
Moderate	0	0	8	4	11	3	26
Severe	0	0	9	8	8	1	26
Total	2	0	32	14	36	10	94

Figure 29 illustrates the age breakdown of DISH and its degrees of severity. Diffuse idiopathic skeletal hyperostosis, while age related, is more prevalent in the 50 to 79 year old age range.

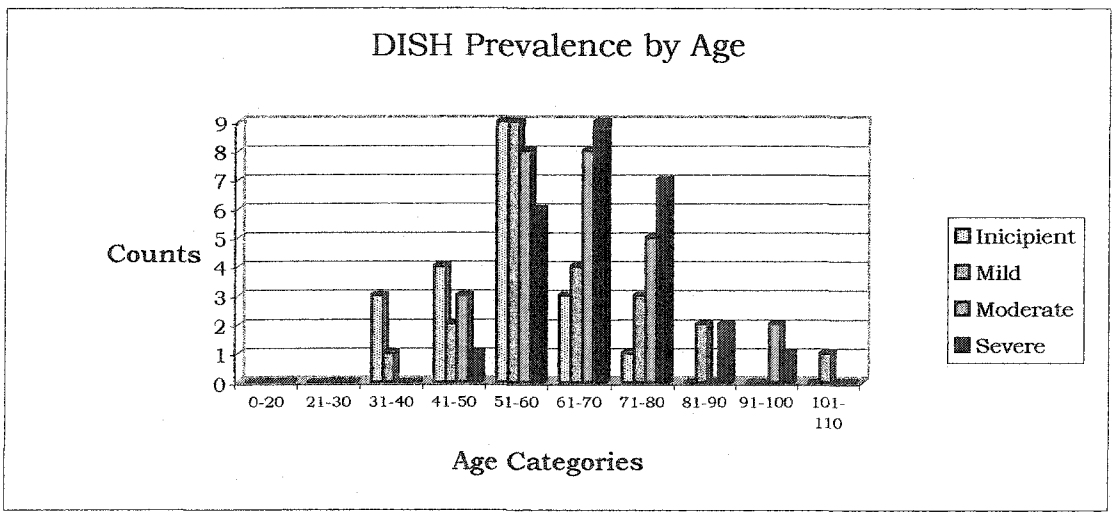

Fig. 29. DISH prevalence by age categories.

Figure 30 graphically shows the number of individuals within each age range in the entire Terry Collection, DISH affected individuals included. This figure is included so the age ranges of DISH prevalence can be compared to the age ranges of the collection as a whole.

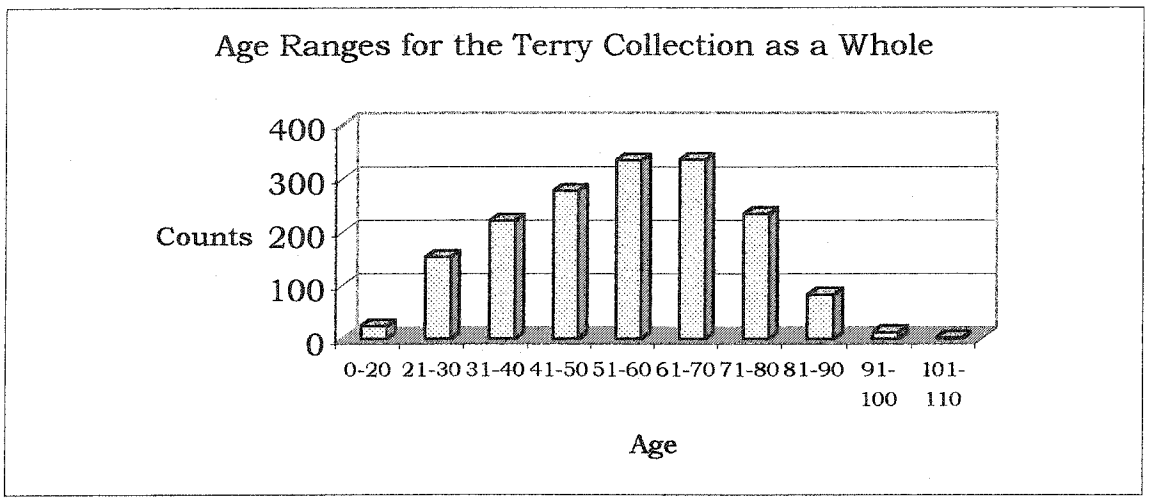

Fig. 30. Age ranges for the Terry Collection as a whole.

Correlation results

This research revealed several strong correlations between the amount of DISH ossification expressed in the body and age. An absolute r value of 0.600 or greater with a corresponding p value of less than 0.05 was considered significant. Table 11 lists the elements with the best correlations. For a list of all correlations, see APPENDIX II.

TABLE 11. Elements with enthesopathies that correlate best with age

Element	
Linea Aspera	Greater Trochanter
Infraglenoid Fossa	Tibial Spines
Acromion	Superior Calcaneus
Olecranon	Radial Tuberosity

Spinal regression results

Males: all categories. Multiple sets of regression equations have been created based on spinal information. The first set pools the information from all DISH degree of severity categories, controlling for sex, and creates a regression equation based on this data. Using the length and the width of the spinal ossification, the equation is able to account for 37% of the variance within the data. The p value for length is 0.7423 and the p value for width is 0.0015. The p value for the model as a whole is $p > 0.0003$. The equation is:

Age = 44.23 + 0.01 x Length + 0.73 x Width

Obviously width is the more reliable measurement but when used in the regression by itself, the regression line is still only able to account for 37% of the variance. However, the p value becomes more reliable with a value of <0.0001. The p value for the model as a whole is $p > 0.0001$. The equation is:

Age = 44.13 + 0.77 x Width

In both cases the sample size is 38.

Males: incipient and mild categories. Unfortunately, sample size became a problem so instead of creating regression equations for every category of DISH, which would have been ideal, the author was forced to pool categories. Thus regressions were run on the combined groups of incipient and mild DISH sufferers. When length and width are used, the equation is able to account for only 36% of the variance in the data. Length has a p value of 0.8826 and width has a p value of 0.0623. The model as a whole has a p value of 0.1363. The equation is:

Age = 43.73 + 0.03 x Length + 0.74 x Width

Again, width is the more telling aspect of the ossification. When width alone is used in the regression, the R-square value is 42%. The probability of the model as a whole is $p > 0.0405$. The equation is:

Age = 44.12 + 0.75 x Width

In both cases the sample size is 12.

Males: moderate and severe categories. Using vertebral ossification length and width, the regression has an R-square value of 11%. The p value of the length is 0.7861 and the p value of the width is 0.1326. The probability of the model as a whole is $p > 0.2743$. The equation is:

Age = 44.77 + 0.11 x Length + 0.71 x Width

As with the other categories, width is a more useful marker in accounting for the data than length.

When width is used in a simple linear regression equation, the R-square value is 11%, the p value for width is 0.1091 and the probability for the model as a whole is $p > 0.1091$. The equation is:

Age = 45.38 + 0.73 x Width

In both cases the sample size is 26.

Females: all categories. When only length and width are used in the regression formula the R-square value is 16%. The p value of length is 0.2870 and the p value of width is 0.2860. The p value for the model as a whole is $p > 0.3606$. The equation is:

Age = 67.23 - 0.08 x Length + 0.41x Width

Width by itself gives an R-square value of 7% and a p value of 0.3440. The probability of the model as a whole is $p > 0.3440$. The equation is:

Age = 60.74 + 0.36 x Width

The sample size in both cases is 15.

Females: incipient and mild categories. Only two females were present thus making sample size a problem even when the incipient and mild categories were pooled. As a result no equations could be created for this category.

Females: moderate and severe categories. When ossification length and width are used in the regression formula, R-square equals 30%. The p value of length is 0.7221 and the p value of width is 0.1067. The probability of the model as a whole is $p > 0.2437$. The equation is:

Age = 44.02 + 0.03 x Length + 0.66 x Width

When only width is used in the regression, the R-square value is 29%. The p value of width is 0.0904 and the probability of the model as a whole is $p > 0.0904$. The equation is:

Age = 49.63 + 0.61 x Width

The sample size in both cases is 11.

Extraspinal and spinal regression results

The percentages for all of the spinal regressions are quite low so the logical next step is to add information from the extraspinal measurements to the spinal regressions in an effort to boost the R-square values.

Males: incipient and mild categories. After adding extraspinal data to the spinal data, the multiple regression equation has an R-square value of 52%. The equation is:

Age = 38.71 + 1.57 x Width of spinal ossification + 0.12 x Soleal line - 0.01 x Linea aspera – 0.19 x Olecranon – 0.01 x Patella

R-Squ = 0.52 p > 0.0716 n = 12

Figure 31 graphically illustrates the regression line for this equation.

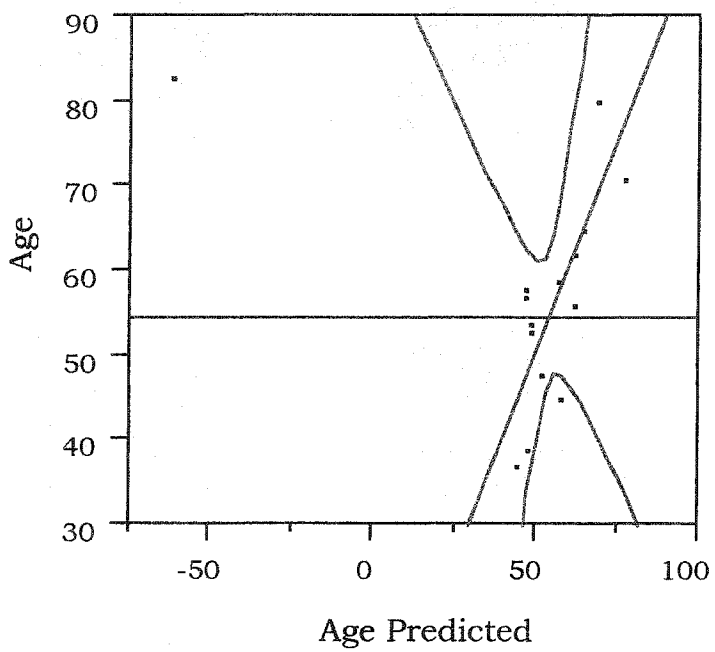

Fig. 31. Regression line for incipient/mild males.

Males: moderate and severe categories. The multiple regression equation created for this category has an R-square value of 41%. The equation is as follows:

Age = 42.61 + 0.84 x Width of spinal ossification + 0.73 x Acromion + 0.02 x Bicipital groove – 0.01 x Patella – 0.12 x Superior calcaneus

R-Squ = 0.41 p > 0.0483 n = 26

Figure 32 illustrates the regression line for this equation.

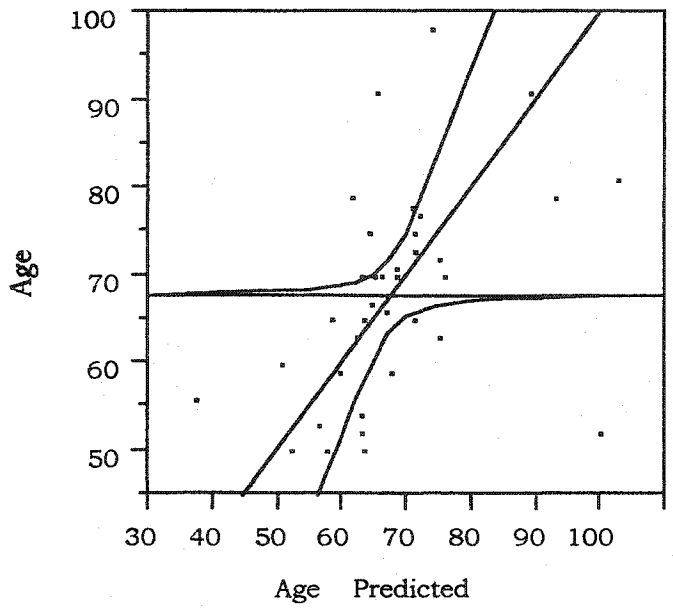

Fig. 32. Regression line for moderate/severe males.

Females: all categories. When combining spinal and extraspinal elements, the regression equation has an R-square value of 85%. The equation is:

Age = 49.45 + 0.50 x Width of spinal ossification – 0.19 x Acromion + 0.15 x Olecranon + 0.05 x Inferior calcaneus + 0.01 x Patella

R-Squ = 0.85 p > 0.0034 n = 15

Figure 33 illustrates the regression line for this equation.

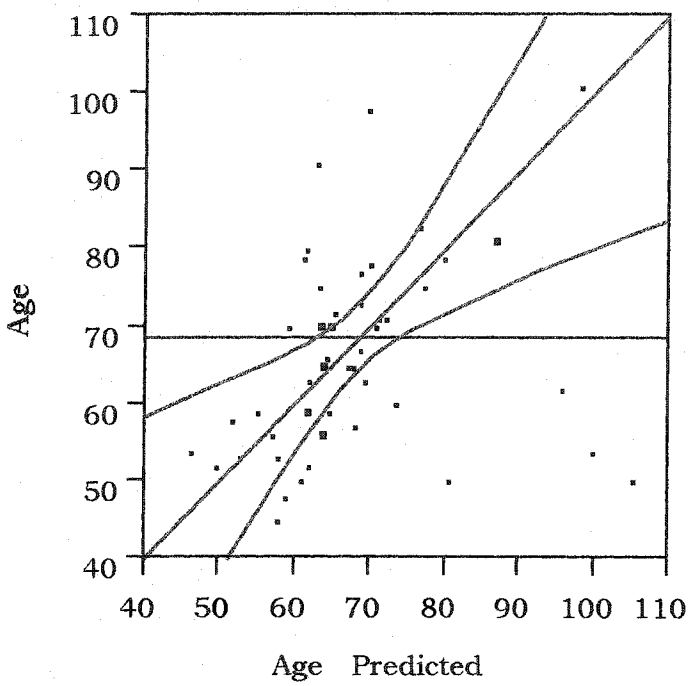

Fig. 33. Regression line for all DISH degrees females.

Females: incipient and mild categories. As with the spinal regressions, the sample size for this category was too small to run regression statistics on.

Females: moderate and severe categories. The regression equation created for this category has an R-square value of 91%. The equation is as follows:

Age = 47.82 + 0.56 x Width of spinal ossification – 42.21 x Infraglenoid fossa + 4.38 x Bicipital groove + 0.37 x Olecranon – 0.10 x Superior Calcaneus

R-Squ = 0.91 p > 0.0166 n = 11

Figure 34 illustrates the regression line for this equation.

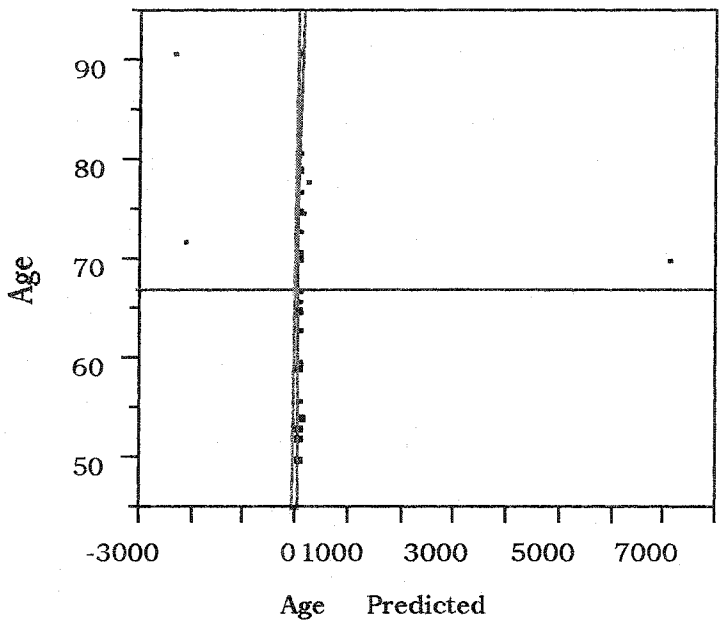

Fig. 34. Regression line for moderate/severe females.

CHAPTER 5

DISCUSSION

This thesis uncovered many very strong correlations between DISH and age at death. It was able to produce regression equations that allow age predictions based on the level of DISH seen in the skeleton, and it was able to validate a scoring system that this author suggests be the standard scoring system used whenever DISH is present in skeletal populations.

Discussion of regression results

General results. The low R-square values for the regressions when considering all categories as a whole was not unexpected. The mixing of incipient and mild categories with moderate and severe ones could only throw off the results because while a 100 year old could have an incipient or mild case of DISH, a 40 year old would not have a moderate or severe case of DISH.

The low R-square values for the regressions relying only on spinal data were not completely unexpected, yet still disappointing in that it

would have been preferable to keep the final regression equations as simple as possible.

The unexpected results came from the extraspinal data. Those who have analyzed a number of individuals with DISH have no doubt noticed the extreme enthesopathies in areas such as the iliac crest. It was expected that the enthesopathies in this regions would be the most diagnostic when it came to establishing an age at death and yet it was among the least useful in this effort as it showed low correlations with age. Instead, enthesopathies in unexpected areas such as the infraglenoid fossa, acromion, and medial epicondyle were more indicative of age at death.

Specific results. While many regression equations were created as a part of this project, the author recommends only very specific ones be used. None of the equations incorporating only data from spinal ossification measurements produced high enough R-square values to warrant ever using them. Therefore, only the equations integrating spinal and extraspinal data should be considered. Because chi square tests indicated significant differences between males and females, separate equations should be used for both sexes. The elements used in the final equations were chosen because they increased the R-square values for each equation, correlated well with age at death, and had a

high correlation when testing for bilaterality (thus ensuring DISH was being measured and not other hyperostotic conditions).

Recommended equations for males. Sample sizes were such that the equations created for both the incipient/mild category and the moderate/severe category are valid. As has been stated, equations based on spinal data alone are not useful; therefore, if a male has either incipient or mild DISH then the following equation should be used:

Age = 38.71 + 1.57 x Width of spinal ossification + 0.12 x Soleal line - 0.01 x Linea aspera – 0.19 x Olecranon – 0.01 x Patella

R-Squ = 0.52 p > 0.0716 n = 12

The equation accounts for 52% of the variance within the data.

If a male has either moderate or severe DISH then the recommended equation is:

Age = 42.61 + 0.84 x Width of spinal ossification + 0.73 x Acromion + 0.02 x Bicipital groove – 0.01 x Patella – 0.12 x Superior calcaneus

R-Squ = 0.41 p > 0.0483 n = 26

This equation accounts for 41% of the variance within the data.

Recommended equations for females. As with males, equations based solely on spinal ossification measurements are not reliable enough to use, but those equations using spinal and extraspinal measurements

are. Unfortunately the sample size for the incipient/mild category was too small to create an equation, so the author recommends using the equation created for females in all categories combined when dealing with a female with an incipient or mild case of DISH. The equation is:

Age = 49.45 + 0.50 x Width of spinal ossification – 0.19 x Acromion + 0.15 x Olecranon + 0.05 x Inferior calcaneus + 0.01 x Patella

R-Squ = 0.85 p > 0.0034 n = 15

The equation is not the ideal, however, it does account for 85% of the variance in the data.

If dealing with females in the moderate or severe categories, the recommended equation is:

Age = 47.82 + 0.56 x Width of spinal ossification – 42.21 x Infraglenoid fossa + 4.38 x Bicipital groove + 0.37 x Olecranon – 0.10 x Superior Calcaneus

R-Squ = 0.91 p > 0.0166 n = 11

The equation accounts for 97% of the variance within the data and thus is reliable.

An illustrated example of using DISH to estimate age at death

Case: Smithsonian Institution, Terry Collection #16RR

Sex: Female Level of DISH: Moderate (Fig. 35)

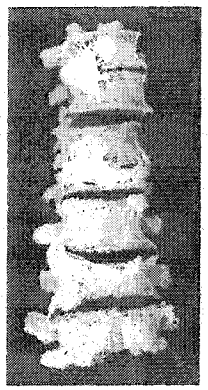

Fig. 35. Smithsonian Institution, Terry Collection #16RR: Moderate DISH.

The appropriate equation for females with moderate DISH is:

Age = 47.82 + 0.56 x Width of spinal ossification – 42.21 x Infraglenoid fossa + 4.38 x Bicipital groove + 0.37 x Olecranon – 0.10 x Superior Calcaneus

Table 12 lists the ossification measurements necessary for this equation.

TABLE 12. Measurements needed for females with moderate DISH

Elements and Measurements		
Width of spinal ossification	=	32.70
Infraglenoid fossa	=	0 (non DISH related pathology)
Bicipital groove	=	5.62
Olecranon	=	0 (non DISH related pathology)
Superior calcaneus	=	13.85

Age = 47.82 + (0.56 x 32.70) – (42.21 x 0) + (4.38 x 5.62) + (0.37 x 0) – (0.10 x 13.85)

Age = 47.82 + 18.31 – 0 + 24.62 + 0 – 1.39

Age = 89.36

Actual age according to Terry Collection records: 91

Strengths and weaknesses of the thesis

Strengths. There are many strong points in the methodology and execution of this research. Foremost among the strengths is the fact that a population of known age, sex, and biological affinity was used for data gathering; therefore, the errors intrinsic in osteological biological profiling methods are not imbedded in the aging methodology created by this research. Another strong point of the aging methodology is that the measurements required to use the regression equations are metric and therefore are less vulnerable to subjective interpretation. Finally, the DISH scoring system tested in this thesis was successful and can be used in any individual exhibiting DISH ossification, regardless of antiquity or ethnic population.

Weaknesses. This research suffers from its small sample size and from the problems inherent in studying only one population and then attempting to create a methodology that will apply to every population on earth. The author is fully aware of the dangers of using metric

measurements taken from a modern population and using regression equations based on such data in archaeological populations. The author proposes that the aging technique is more useful in forensic settings but perhaps once more research is complete (i.e. the technique is studied in various archaeological populations) it can be used with fewer reservations when dealing with ancient skeletons. The author further recognizes that females were greatly underrepresented in this study. While females have been thought to be half as likely as males to have DISH, the author nonetheless acknowledges the need for a greater female sample size to create the best regression equations possible for females with DISH.

Further research

There was an attempt on the author's part to establish an intraobserver error percentage; however, time and budget restrictions prevented her from doing so in the manner in which she had hoped (i.e. go through the entire Terry Collection twice, diagnosing, scoring, and measuring DISH blindly both times). Instead, she was only able to analyze a limited number of randomly chosen individuals twice and infer an intraobserver error from that. In addition to intraobserver error, interobserver error would be a very interesting study; how well can others replicate this technique? The author believes the replicability will

be high; however, it would add strength to the aging methodology if another researcher were to replicate this author's findings.

Once all issues of replicability and sample size are resolved, the method should be tested on various populations from around the world to see if the equations need to be modified depending on the biological affinity of the population under study. If multiple populations were analyzed then researchers would also know if the regression equations are population specific or if they are more universal.

Summary and final thoughts

The first step in using this methodology is to diagnose DISH in an individual and score the severity of the condition based on the scoring system defined in this thesis. Next, sex the individual because there are significant differences between males and females when it comes to diffuse idiopathic skeletal hyperostosis. Once the degree of DISH severity and the sex of the individual have been established, use the regression equation that corresponds to the overall category in which the individual falls. Use the equation to determine which ossification measurements need to be taken. Solve the equation and it will produce an estimated age at death for the individual.

It is unfortunate that the multiple regression equations for males in both categories had such low R-square values. However, because of the small sample size, this should be considered a preliminary study, the

results of which are promising enough to warrant further research and should not deter workers from using the equations. Overall the author believes this is a good methodology for assessing age at death. It will probably never replace the pubic symphysis as the most reliable method created, but when used on females it is on par with many other techniques in general use and should be considered as another tool with which to gather information whenever a researcher encounters a skeleton with signs of diffuse idiopathic skeletal hyperostosis.

LITERATURE CITED

Anderson KN, Anderson LE, and Glanze WD. 1998. Mosby's Medical, Nursing, & Allied Health Dictionary. 5th Edition. St Louis MO: Mosby.

Arnet FC. 1997. Ankylosing spondylitis. In: Koopman WJ, editor. Arthritis and allied conditions: A Textbook of Rheumatology 13th Edition Volume 1. Baltimore: Williams & Wilkins. p 1197-1208.

Arriaza BT. 1991. The search for seronegative spondyloarthropathies and diffuse idiopathic skeletal hyperostosis in ancient South America. Dissertation, Arizona State University.

Arriaza BT. 1993. Seronegative spondyloarthropathies and diffuse idiopathic skeletal hyperostosis in ancient Northern Chile. Am J Phys Anthropol 91:263-278.

Arriaza BT. 2000. DISH and age. Paper presented at the San Diego Forensic Meeting, in San Diego, CA. October 7, 2000.

Arriaza BT, Merbs CF, and Rothschild BM. 1993. Diffuse idiopathic skeletal hyperostosis in Meroitic Nubians from Semna South, Sudan. Am J Phys Anthropol 92:243-248.

Aufderheide AC, and Rodríguez-Martín C. 1998. The Cambridge encyclopedia of human paleopathology. Cambridge: Cambridge University Press.

Ball J. 1971. Enthesopathy of rheumatoid and ankylosing spondylitis. Ann Rheum Dis 30:213-223.

Bass WM, Gregg JB, and Provost PE. 1974. Ankylosing spondylitis (Marie Strumpel disease) in historic and prehistoric northern Plains Indians. Plains Anthropologist 19(66):303-305.

Benjamin M, Rufai A, and Ralphs JR. 2000. The mechanism of formation of bony spurs (enthesophytes) in the achilles tendon. Arthritis & Rheumatism 43(3):576-583.

Bennett RM. 1997. Psoriatic arthritis. In: Koopman WJ, editor. Arthritis and allied conditions: a textbook of rheumatology 13th Edition Volume 1. Baltimore: Williams & Wilkins. p 1229-1244.

Beyeler C, Schlapbach P, Gerber NJ, Sturzenegger J, and Fahrer H. 1990. Diffuse idiopathic skeletal hyperostosis (DISH) of the shoulder: a cause of shoulder pain? Br. J. Rheumatol 29:349-353.

Blondiaux J, Cotten A, Fontaine C, Hänni C, Bera A, and Flipo R. Two Roman and medieval cases of symmetrical erosive polyarthropathy from Normandy: anatomico-pathological and radiological evidence for reumatoid arthritis. Int J Osteoarchaeol 7:451-466.

Bourke JB. 1967. A rview of the paleopathology of the arthritic diseases. In: Brothwell D, and Sandison AT, editors. Diseases in antiquity: a survey of the diseases, injuries and surgery of early populations. Springfield: C.C. Thomas Springfield. p 352-360.

Brandt J, Haibel H, Cornely D, Golder W, Gonzalez J, Reddig J, Thriene W, Sieper J, and Braun J. 2000. Successful treatment of active ankylosing spondylitis with the anti-tumor necrosis factor α monoclonal antibody infliximab. Arthritis & Rheumatism 43(6):1346-1352.

Bridges PS. 1991. Degenerative joint disease in hunter-gatherers and agriculturalists from the southeastern United States. Am J Phys Anthropol 85:379-391.

Bridges PS. 1994. Vertebral arthritis and physical activities in the prehistoric southeastern United States. Am J Phys Anthropol 93:83-93.

Brigode M, Francois RJ, and Dory MA. 1982. Radiological study of the sacroiliac joints in vertebral ankylosing hyperostosis. Ann Rheum Dis 41:225-231.

Buikstra JE, and Ubelaker DH. 1994. Standards for data collection from human skeletal remains. Arkansas: Arkansas Archaeological Survey.

Bywaters EGL. 1983. Historical perspectives in the aetiology of ankylosing spondylitis. British Journal of Rheumatology 22(suppl 2): 1-4.

Casas MJ, Crubezy E, Haye L, and Briois. 1996. Degnerative joint disease and enthesopathies in a Bronze Age population from Sindou Cave (Senaillac-Lauzes, Lot, France). Human Evolution 11(2):147-158.

Chapman FH. 1972. Vertebral osteophytosis in prehistoric populations of central and southern Mexico. Am J Phys Anthropol 36:31-38.

Corathay A, Hansson AS, and Homdahl R. 2000. T lymphocytes are not required for the spontaneous development of entheseal ossification leading to marginal ankylosis in the DBA/1 Mouse. Arthritis & Rheumatism 43(4):844-851.

Crubézy E. 1990. Diffuse idiopathic skeletal hyperostosis: diagnosis and Importance in paleopathology. Journal of paleopathology 3(2):107-118.

Crubézy E, and Trinkaus E. 1992. Shanidar 1: a case of hyperostotic disease (DISH) in the middle paleolithic. Am J Phys Anthropol 89:411-420.

Cush JJ, and Lipsky PE. 1997. Reiter's syndrome and reactive arthritis. In: Koopman WJ, editor. Arthritis and allied conditions: a textbook of rheumatology 13th Edition Volume 1. Baltimore: Williams & Wilkins. p 1209-1227.

DeRousseau CJ. 1985. Ageing in the musculoskeletal system of rhesus monkeys: II. degenerative joint disease. Am J Phys Anthropol 67:177-184.

Dougados M, van der Linden S, Juhlin R, Huitfeldt B, Amor B, Calin A, Cats A, Dijkmans B, Olivieri I, Pasero G, Veys E, Zeidler H, and The European Spondylarthropathy Study Group. 1991. The European spondylarthropathy study group preliminary criteria for the classification of spondylarthropathy. Arthritis & Rheumatism 34(10):1218-1230.

Dutour O. 1986. Enthesopathies (lesions of muscular insertions) as indicators of the activities of Neolithic Saharan Populations. Am J Phys Anthropol 71:221-224.

Ekman P, Kirveskari J, and Granfors K. 2000. Modification of disease outcome in salmonella-infected patients by HLA-B27. Arthritis & Rheumatism 43(7):1527-1534.

Fairgrieve SI. 1999. Forensic osteological analysis. Illinois: Charles C. Thomas.

Forestier J, and Rotes-Querol J. 1950. Senile ankylosing hyperostosis of the spine. Ann Rheum Dis 24:321-330.

Forestier J, and Lagier R. 1971. Ankylosing hyperostosis of the spine. Clin Orthop 74:65-83.

François RJ, Gardner DL, Degrave EJ, and Bywaters EGL. 2000. Histopathologic evidence that sacroilitis in ankylosing spondylitis is not merely enthesitis: systematic study of specimens from patients and control subjects. Arthritis & Rheumatism 43(9): 2011-2024.

Gratacós J, Collado A, Pons F, Osaba M, Sanmartí R, Roqué M, Larrosa M, and Múñoz-Gómez. 1999. Significant loss of bone mass in patients with early, active ankylosing spondylitis. Arthritis & Rheumatism 42(11):2319-2324.

Gray H. 1956. Anatomy of the human body. Gross CM ed. Philadelphia PA: Lea & Febiger.

Hall-Craggs EB. 1990. Anatomy as a basis for clinical medicine. 2nd Edition. Baltimore: Urban & Schwarzenberg.

Hammer RE, Maika SD, Richardson JA, Tang J, and Taurog JD. 1990. Spontaneous inflammatory disease in transgenic rats expressing HLA-B27 and human β_2m: an animal model of HLA-B27-associated human disorders. Cell 63:1099-1112.

Hajkova Z, Streda A, and Skrha F. 1965. Hperostotic spondylosis and diabetes mellitus. Ann Rheum Dis 24:536-543.

Hawkey DE and Merbs CF. 1995. Activity-induced musculoskeletal stress markers (MSM) and subsistence strategy changes among ancient Hudson Bay Eskimos. Int J Osteoarchaeol 5:324-338.

Hoyle E, Laval SH, Calin A, Wordsworth BP, and Brown MA. 2000. The x-chromosome and susceptibility to ankylosing spondylitis. Arthritis & Rheumatism 43(6):1353-1355.

Hukuda S, Inoue K, Ushiyama T, Saruhashi Y, Iwasaki A, Huang J, Mayeda A, Nakai M, Li FX, and Yang ZQ. 2000. Spinal degenerative lesions and spinal ligamentous ossifications in ancient Chinese populations of the Yellow river civilization. Int J Osteoarchaeol 10:108-124.

Hunt D. 2000. History of the Robert J. Terry anatomical skeletal collections. Internet.

Hunter T. 1989. The spinal complications of ankylosing spondylitis. seminars. Arthritis & Rheumatism 19(3):172-182.

Julkunen H, Heinonen OP, Knekt P, and Maatela J. 1975. The Epidemiology of hyperostosis of the spine together with its symptoms and related mortality in a general population. Scand J Rheum 4:23-27.

Jurmain R. 1977. Stress and the etiology of osteoarthritis. Am J Phys Anthropol 46:353-366.

Jurmain R. 1990. Paleoepidemiology of a central California prehistoric population from CA-ALA-329: II. degenerative disease. Am J Phys Anthropol 83:83-94.

Kahl KE, and Smith MO. 2000. The pattern of spondylosis deformans in prehistoric samples from west-central New Mexico. Int J Osteoarchaeol 10:432-446.

Kidd KE. 1954. A note on the paleopathology of Ontario. Am J Phys Anthropol 12:610-613.

Klepinger LL. 1979. Paleopathologic evidence for the evolution of rheumatoid arthritis. Am J Phys Anthropol 50:119-122.

Knüsel CJ, Göggel S, and Lucy D. 1997. Comparative degenerative joint disease of the vertebral column in the medieval monastic cemetery of the Gilbertine prior of St. Andrew, Fishergate, York, England. Am J Phys Anthropol 103:481-495.

Lagier R. 1989. Spinal hyperostosis in comparative pathology. Skeletal Radiol 18:99-107.

Littlejohn GO, Urowitz MB, Smythe HA, and Keystone EC. 1981. Radiographic features of the hand in diffuse idiopathic skeletal hyperostosis (DISH): comparison with normal subjects and acromegalic patients. Radiology 140:623-629.

Mann RW, and Murphy SP. 1990. Regional atlas of bone disease: a guide to pathological and normal variation in the human skeleton. Illinois: Charles C. Thomas Publisher.

Maat GJR, Mastwijk RW, and Van Der Velde EA. 1995. Skeletal distribution of degenerative changes in vertebral osteophytosis, vertebral osteoarthritis and DISH. Int J Osteoarchaeol 5:289-298.

Martínez-Borra J, González S, and López-Larrea C. 2000. Genetic factors predisposing to spondylarthropathies. Arthritis & Rheumatism 43(3):485-492.

McEwen C, DiTat D, Lingg C, Porini A, Good A, and Rankin T. 1971. Ankylosing spondylitis and spondylitis accompanying ulcerative colitis, regional enteritis, psoriasis and Reiter's disease: a comparative study. Arthritis & Rheumatism 14(3):291-318.

Merbs CF. 1983. Patterns of activity induced pathology in a Canadian Inuit population. Ottawa: Archaeological Survey of Canada. National Museum of Man, Mercury series 119.

Oppenheimer A. 1942. Calcification and ossification of vertebral ligaments (spondylitis ossificans ligamentosa): roentgen study of pathogenesis and clinical significance. Radiology 38:160-164.

Ortner DJ, and Putschar WGJ. 1985. Identification of pathological conditions in human skeletal remains. Washington, DC: Smithsonian Institution.

Ortner DJ. 1987. Archaeological evidence of polyarticular inflammatory arthritides in North America. In: Appelboom T, editor. Art, history and antiquity of rheumatic diseases. Brussels: Elsevier Brussels. 92-97.

Resnick D. 1985. Degenerative diseases of the vertebral column. Radiology 156:3-14.

Resnick D, Mitchell L, Feingold DM, Curd J, Niwayama G, and Goergen TM. 1977. Calcaneal abnormalities in articular disorders. Radiology 125:355-366.

Resnick D, and Niwayama G. 1976. Radiographic and pathologic features of spinal involvement in diffuse idiopathic skeletal hyperostosis (DISH). Radiology 119:559-568.

Resnick D, and Niwayama G. 1983. Entheses and enthesopathy. Radiology 146:1-9.

Resnick D and Niwayama G. 1995. Degenerative disease of the spine. In: Diagnosis of bone and joint disorders 3rd Edition. Philadelphia: Saunders WB. p 1372-1412.

Resnick D, Shaul SR, and Robins JM. 1975. Diffuse idiopathic skeletal hyperostosis (DISH): Forestier's disease with extraspinal manifestations. Radiology 115:513-524.

Rogers J, Watt I, and Dieppe P. 1985. Palaeopathology of spinal osteophytosis, vertebral ankylosis, ankylosing spondylitis, and vertebral hyperostosis. Ann Rheum Dis 44:113-120.

Rogers J, Waldron T, Dieppe P, and Watt I. 1987. Anthropathies in palaeopathology: the basis of classification according to most probable cause. Journal of Archaeological Science 14:179-193.

Rothschild BM. 1988. Diffuse idiopathic skeletal hyperostosis. Comprehensive Therapy 14(2):65-69.

Rothschild BM, Arriaza B, Woods RJ, and Dutour O. 1999. Spondyloarthropathy identified as the etiology of nubian erosive arthritis. Am J Phys Anthropol 109:259-267.

Rothschild BM, and Woods RJ. 1989. Spondyloarthropathy in gorillas. Seminars in Arthritis and Rheumatism 18(4):267-276.

Rothschild BM, and Woods RJ. 1991. Arthritis in an early 20th century geriatric population. Age 14:17-19.

Rothschild BM and Woods RJ. 1992. Erosive arthritis and spondyloarthropathy in Old World primates. Am J Phys Anthropol 88:389-400.

Said-Nahal R, Miceli-Richard C, Berthelot JM, Duché A, Dernis-Labous E, Le Blévec G, Saraux A, Perdriger A, Guis S, Claudepierre P, Sibilia J, Amor B, Dougados M, and Breban M. 2000. The Ffmilial form of spondylarthropathy: a clinical study of 115 multiplex families. Arthritis & Rheumatism. 43(6):1356-1365.

Schmorl G. 1971. The human spine in health and disease. 2nd American Edition. Besemann EF ed. New York: Grune & Stratton.

Schwartz JH. 1995. Skeleton keys: an introduction to human skeletal morphology, development, and analysis. Oxford: Oxford University Press.

Shaibani A, Workman R, and Rothschild BM. 1993. The significance of enthesopathy as a skeletal phenomenon. Clinical and Experimental Rheumatology 11:399-403.

Smith SD, Smith SB, Young-Paden B, and Ellis WN. 1994. Fatigue perturbation of the os calcis. The Journal of Foot and Ankle Surgery 33(4):402-410.

Sobao Y, Tsuchiya N, Takiguchi M, and Tokunaga K. 1999. Overlapping peptide-binding specificities of HLA-B27 and B39: evidence for a role of peptide supermotif in the pathogenesis of spondylarthropathies. Arthritis & Rheumatism 42(1):175-181.

Sofaer Darevenksi JR. 2000. Sex differences in activity-related osseous change in the spine and the gendered division of labor at Ensay and Wharram Percy, UK. Am J Phys Anthropol 111:333-354.

Suzuki T, Fujita H, Narasaki S, Kondo O, Adachi K. 1993. A study of skeletal remains with diffuse idiopathic skeletal hyperostosis (DISH) from the Edo period, Japan. Anthropol Sci 101(3):273-290.

Tyrdal S, and Finnager AM. 1999. Osseous manifestations of 'handball goalie's elbow'. Scand J Med Sci Sports 9:92-97.

Utsinger PD. 1985. Diffuse idiopathic skeletal hyperostosis. Clinics Rheumat Dis 11:325-351.

Van der Linden S, Valkenburg HA, and Cats A. 1984. Evaluation of diagnostic criteria for ankylosing spondylitis. Arthritis & Rheumatism 27(4):361-368.

Vittecoq O, Said LA, Michot C, Mejjad O, Thomine JM, Mitrofanoff P, Lechevallier J,Ledosseur P, Gayet A, Lauret P, and LE Loët X. 2000. Evolution of chronic recurrent multifocal osteitis toward spondylarthropathy over the long term. Arthritis & Rheumatism 43(1):109-119.

Weinreich S, Eulderink F, Capkova J, Pla M, Gaede K, Heesemann J, van Alphen L, Zurcher C, Hoeve-Hewryk B, Kievits F, and Ivanyi P. 1995. HLA-B27 as a relative risk factor in ankylosing enthesopathy in transgenic mice. Human Immunol 42:103-115.

White TD. 1991. Human osteology. San Diego: Academic Press Inc.

Willkens RF, Arnett FC, Bitter T, Calin A, Fisher L, Ford DK, Good AE, and Masi AT. 1981. Reiter's syndrome: evaluation of preliminary criteria for definite disease. Arthritis & Rheumatism 24(6):844-849.

Woodrow JC. 1985. Genetic aspects of the spondyloarthropathies. Clinics in Rheumatic Diseases 11(1):1-23.

Zias J, and Mitchell P. 1996. Psoriatic arthritis in a fifth-century Judean desert monastery. Am J Phys Anthropol 101:491-502.

Zorab PA. 1961. The historical and prehistorical background of ankylosing spondylitis. Proc. Roy. Soc. Med. 54:415-420.

APPENDIX I

DATA FORMS USED IN THIS THESIS

VERTEBRAE INVENTORY AND EXISTING BIOLOGICAL PROFILE

Collection Name: Terry Collection
Location of Collection: Smithsonian Institution
Catalog Number: _____

Observer: Jennifer Riddle
Date: 2001
Photographs: _____

Inventory

√ = Present
X = Absent

C1 ☐
C2 ☐
C3 ☐
C4 ☐
C5 ☐
C6 ☐
C7 ☐
T1 ☐
T2 ☐
T3 ☐
T4 ☐
T5 ☐
T6 ☐
T7 ☐
T8 ☐
T9 ☐
T10 ☐
T11 ☐
T12 ☐
L1 ☐
L2 ☐
L3 ☐
L4 ☐
L5 ☐

Notes/Drawings

_____
_____
_____
_____
_____
_____
_____
_____
_____
_____
_____
_____

Existing Bio Profile

Sex: _____

Age: _____

Race: _____

Height: _____

Weight: _____

Cause of Death: _____
_____

DISH yes/no: _____
Degree: _____

■ = Areas with DISH

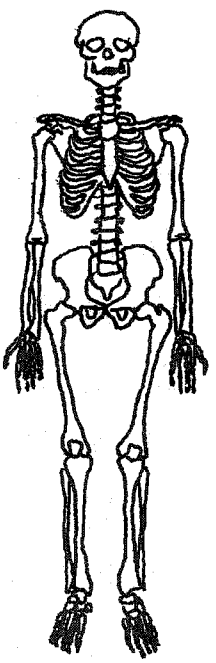

Spurs

Spine with DISH	yes ☐	no ☐
Scapula: Acromion	yes ☐	no ☐
Scapula: Infraglenoid Fossa	yes ☐	no ☐
Humerus: Bicipital Groove	yes ☐	no ☐
Humerus: Deltoid Tubercle	yes ☐	no ☐
Humerus: Medial Epicondyle	yes ☐	no ☐
Ulna: Olecranon Process	yes ☐	no ☐
Radius: Tuberosity	yes ☐	no ☐
Ilium: Crest	yes ☐	no ☐
Femur: Greater Trochanter	yes ☐	no ☐
Femur: Trochanteric Fossa	yes ☐	no ☐
Femur: Lesser Trochanter	yes ☐	no ☐
Patella: Anterior	yes ☐	no ☐
Tibia: Spines	yes ☐	no ☐
Tibia: Soleal Line	yes ☐	no ☐
Calcaneus: Superior	yes ☐	no ☐
Calcaneus: Inferior	yes ☐	no ☐

Other Spinal Pathologies: _____
_____

PRESENCE OF VERTEBRAL OSSIFICATION

Collection: Terry Collection
Catalog Number:
Photograph Number(s):

Observer: Jennifer Riddle
Date: 2001

Anterior View of the Spine

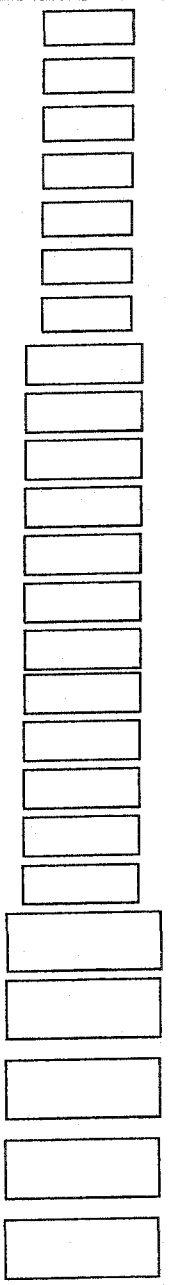

Measurement of the Continuous Ossification

Max Length by Max Width by Left Border Thickness

Block 1 _____

_____

_____

Block 2 _____

_____

_____

Block 3 _____

_____

_____

■ = Ossification of Ligament

Number of Blocks: _____

Vertebrae Involved: _____

PRESENCE OF SCAPULAR OSSIFICATION

Collection Name: Terry Collection
Catalog Number:
Photograph Number(s):

Observer: Jennifer Riddle
Date: 2001

Left

Scapula: Present/Partial/Absent:
DISH: Present/Absent:

■ = Ossification of Ligament

View of the Scapula

Lateral

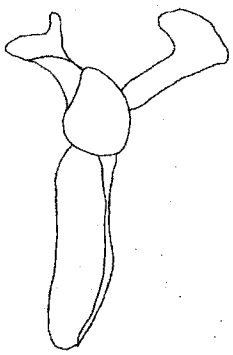

Measurements of the Acromion Ossification

Max Height:
Width:
Thickness:

Measurements of the Infraglenoid Fossa Ossification

Max Height:
Width:
Thickness:

Right

Scapula: Present/Partial/Absent:
DISH: Present/Absent:

■ = Ossification of Ligament

View of the Scapula

Lateral

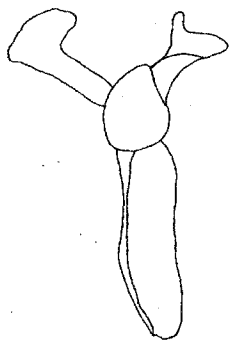

Measurements of the Acromion Ossification

Max Height:
Width:
Thickness:

Measurements of the Infraglenoid Fossa Ossification

Max Height:
Width:
Thickness:

PRESENCE OF PROXIMAL HUMERAL OSSIFICATION

Collection Name: Terry Collection
Catalog Number:
Photograph Number(s):

Observer: Jennifer Riddle
Date: 2001

LEFT

Proximal Humerus: Present/Absent:
DISH: Present/Absent:
■ = Ossification of Ligament

Proximal End of the Humerus

Anterior View

Measurements of the Bicipital Groove Ossification

Max Height:
Width:
Thickness:

Proximal End of the Humerus

Lateral View

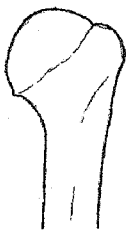

Measurements of the Deltoid Tuberosity Ossification

Max Height:
Width:
Thickness:

RIGHT

Proximal Humerus: Present/Absent:
DISH: Present/Absent:
■ = Ossification of Ligament

Proximal End of the Humerus

Anterior View

Measurements of the Bicipital Groove Ossification

Max Height:
Width:
Thickness:

Proximal End of the Humerus

Lateral View

Measurements of the Deltoid Tuberosity Ossification

Max Height:
Width:
Thickness:

PRESENCE OF DISTAL HUMERAL OSSIFICATION

Collection Name: Terry Collection
Catalog Number:
Photograph Number(s):

Observer: Jennifer Riddle
Date: 2001

LEFT

Distal Humerus: Present/Absent:
DISH: Present/Absent:

■ = Ossification of Ligament

Distal End of the Humerus

Anterior View

Measurements of the Humeral Medial Epicondyle Ossification

Max Height:
Width:
Thickness:

RIGHT

Distal Humerus: Present/Absent:
DISH: Present/Absent:

■ = Ossification of Ligament

Distal End of the Humerus

Anterior View

Measurements of the Humeral Medial Epicondyle Ossification

Max Height:
Width:
Thickness:

PRESENCE OF ULNAR OSSIFICATION

Collection Name: Terry Collection
Catalog Number:
Photograph Number(s):

Observer: Jennifer Riddle
Date: 2001

Left

Proximal Ulna: Present/Absent:
DISH: Present/Absent:

■ = Ossification of Ligament

Proximal End of the Ulna

Medial View Lateral View

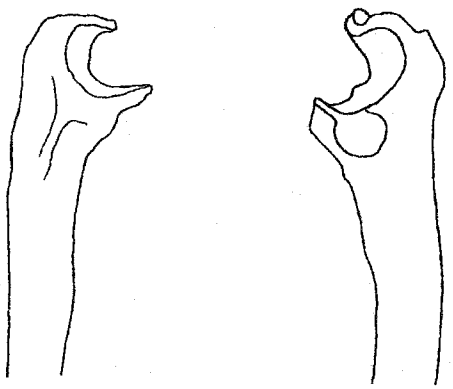

Measurements of the Ulnar Olecranon Ossification

Max Height:
Width:
Thickness:

Right

Proximal Ulna: Present/Absent:
DISH: Present/Absent:

■ = Ossification of Ligament

Proximal End of the Ulna

Medial View Lateral View

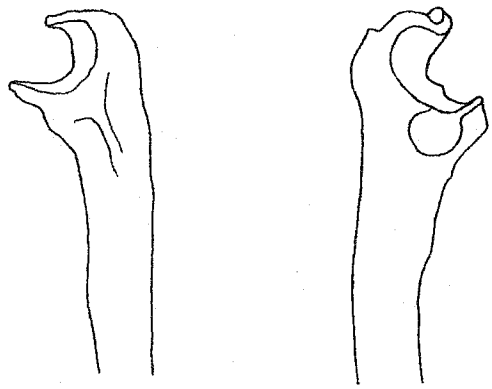

Measurements of the Ulnar Olecranon Ossification

Max Height:
Width:
Thickness:

PRESENCE OF RADIAL OSSIFICATION

Collection Name: Terry Collection
Catalog Number:
Photograph Number(s):

Observer: Jennifer Riddle
Date: 2001

Left

Proximal Radius: Present/Absent:
DISH: Present/Absent:

■ = Ossification of Ligament

Proximal End of the Radius

Medial View

Posterior View

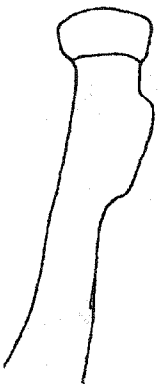

Measurements of the Radial Tuberosity Ossification

Max Height:
Width:
Thickness:

Right

Proximal Radius: Present/Absent:
DISH: Present/Absent:

■ = Ossification of Ligament

Proximal View of the Radius

Medial View

Posterior View

Measurements of the Radial Tuberosity Ossification

Max Height:
Width:
Thickness:

PRESENCE OF ILIAC CREST OSSIFICATION

Collection Name: Terry Collection
Catalog Number:
Photograph Number(s):

Observer: Jennifer Riddle
Date: 2001

Left

Ilium: Present/Absent:
DISH: Present/Absent:

■ = Ossification of Ligament

View of the Ilium

Lateral

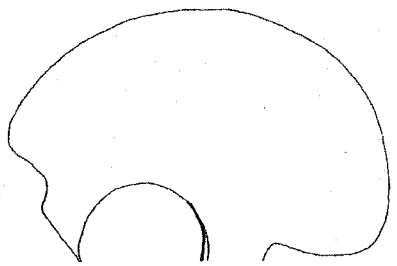

Measurements of the Ossification

Max Height:
Width of the Arc:
Thickness:

Right

Ilium: Present/Absent:
DISH: Present/Absent:

■ = Ossification of Ligament

View of the Ilium

Lateral

Measurements of the Ossification

Max Height:
Width of the Arc:
Thickness:

PRESENCE OF FEMURAL OSSIFICATION

Collection Name: Terry Collection
Catalog Number:
Photograph Number(s):

Observer: Jennifer Riddle
Date: 2001

Left

Proximal Femur: Present/Absent:
DISH: Present/Absent:

■ = Ossification of Ligament

Proximal End of the Femur
Posterior View

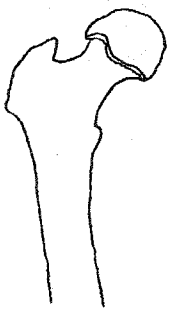

Measurements of the Greater Trochanter Ossification

Max Height:
Width:
Thickness:

Measurements of the Trochanteric Fossa Ossification

Max Height:
Width:
Thickness:

Measurements of the Lesser Trochanter Ossification

Max Height:
Width:
Thickness:

Measurements of the Linea Aspera Ossification

Max Height:
Width:
Thickness:

Right

Proximal Femur: Present/Absent:
DISH: Present/Absent:

■ = Ossification of Ligament

Proximal End of the Femur
Posterior View

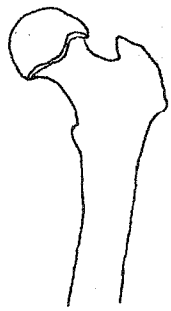

Measurements of the Greater Trochanter Ossification

Max Height:
Width:
Thickness:

Measurements of the Trochanteric Fossa Ossification

Max Height:
Width:
Thickness:

Measurements of the Lesser Trochanter Ossification

Max Height:
Width:
Thickness:

Measurements of the Linea Aspera Ossification

Max Height:
Width:
Thickness:

PRESENCE OF PATELLAR OSSIFICATION

Collection Name: Terry Collection
Catalog Number:
Photograph Number(s):

Observer: Jennifer Riddle
Date: 2001

Left

Patella: Present/Absent:

DISH: Present/Absent:

Anterior View of Patella

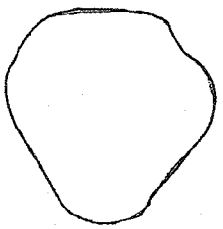

Measurements of the Anterior Ossification

Max Height:
Width:
Thickness:

Right

Patella: Present/Absent:

DISH: Present/Absent:

Anterior View of Patella

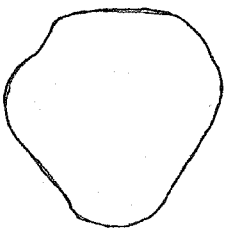

Measurements of the Anterior Ossification

Max Height:
Width:
Thickness:

■ = Ligament Ossification

PRESENCE OF TIBIAL OSSIFICATION

Collection Name: Terry Collection
Catalog Number:
Photograph Number(s):

Observer: Jennifer Riddle
Date: 2001

Left

Proximal Tibia: Present/Absent:
DISH: Present/Absent:

■ = Ossification of Ligament

Proximal End of the Tibia

Posterior View

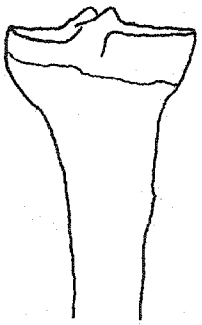

Measurements of the Soleal Line Ossification

Max Height:
Width:
Thickness:

Measurements of the Spinal Ossification

Max Height:
Width:
Thickness:

Right

Proximal Tibia: Present/Absent:
DISH: Present/Absent:

■ = Ossification of Ligament

Proximal End of the Tibia

Posterior View

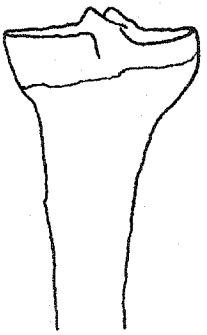

Measurements of the Soleal Line Ossification

Max Height:
Width:
Thickness:

Measurements of the Spinal Ossification

Max Height:
Width:
Thickness:

PRESENCE OF CALCANEAL OSSIFICATION

Collection Name: Terry Collection
Catalog Number:
Photograph Number(s):

Observer: Jennifer Riddle
Date: 2001

Left

Calcaneus: Present/Absent:
DISH: Present/Absent:

■ = Ossification of Ligament

View of the Calcaneus

Dorsal (Superior) Plantar (Inferior)

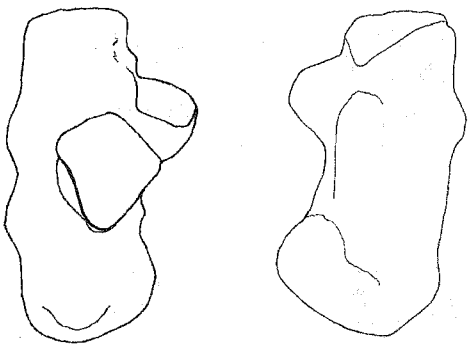

Measurements of the Superior Ossification

Max Height:
Width:
Thickness:

Measurements of the Inferior Ossification

Max Height:
Width:
Thickness:

Right

Calcaneus: Present/Absent:
DISH: Present/Absent:

■ = Ossification of Ligament

View of the Calcaneus

Dorsal (Superior) Plantar (Inferior)

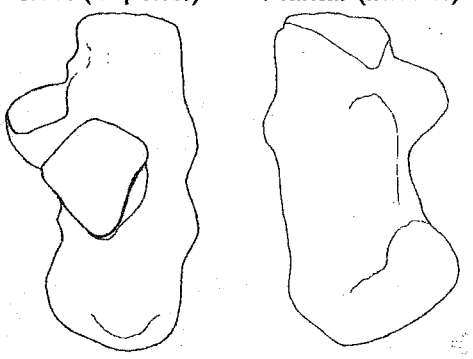

Measurements of the Superior Ossification

Max Height:
Width:
Thickness:

Measurements of the Inferior Ossification

Max Height:
Width:
Thickness:

APPENDIX II

SPINAL AND EXTRASPINAL ELEMENTS CORRELATED WITH AGE

Incipient/mild females: spinal and extraspinal correlations with age

Variable	Age r =
age	1
length	0.5547
width	0.3316
thick	-0.5683
depth	0.0812
vol thick	-0.4834
vol depth	0.083
L acromion	0.8617
L infraglenoid fossa	0.9582
R acromion	-0.8205
R infraglenoid fossa	-0.2469
L biciptial groove	-0.2789
L deltoid tuberosity	0.1674
R bicipital groove	-0.2786
R deltoid tuberosity	0.1674
L epicondyle	0.1787
R epicondyle	0.0362
L olecronon	0.8403
R olecronon	0.8446

L radial tuberosity	0.9217
R radial tuberosity	0.4966
L ilium	-0.0134
R ilium	-0.175
L greater troch	0.9375
L lesser troch	0.8374
L linea aspera	0.5111
R greater troch	-0.0899
R lesser troch	0.9494
R linea aspera	0.4175
L patella	0.3081
R patella	0.2801
L soleal	0.3822
L spine	0.0954
R soleal	-0.1756
R spine	0.6745
L sup calcaneus	-0.6136
L infer calcaneus	-0.2098
R sup calcaneus	0.8662
R infer calcaneus	0.4597

Moderate/severe females: spinal and extraspinal correlations with age

Variable	Age r =
Age	1.0000
length	0.2740
width	0.5812
thick	0.3359
depth	0.5546
vol thick	0.3720
vol depth	0.6463
L acromion	-0.1047
L infraglenoid fossa	0.5461
R acromion	-0.2884
R infraglenoid fossa	0.5943
L bicip groove	0.5461
L deltoid tub	0.5461
R bicip groove	0.5478
R deltoid tub	0.5461
L epicondyle	-0.1635
R epicondyle	0.3908
L olecronon	0.4663
R olecronon	0.5026

L radial tub	0.5331
R radial tub	0.0818
L ilium	0.0496
R ilium	-0.0477
L Great trochanter	0.4602
L less trochanter	-0.4687
L linea aspera	-0.0755
R greater trochanter	0.5348
R less trochanter	0.4366
R linea aspera	0.6355
L patella	0.3926
R patella	0.3399
L soleal	-0.1530
L spine	0.2089
R soleal	-0.0671
R spine	0.4989
L sup calcaneus	-0.4521
L infer calcaneus	-0.2554
R sup calcaneus	-0.5900
R infer calcaneus	-0.2310

Incipient/mild males: spinal and extraspinal correlations with age

Variable	Age r =
age	1.0000
length	0.1869
width	0.5968
thick	-0.0366
depth	0.2435
vol thick	0.3141
vol depth	0.2452
L acromion	-0.2032
L infraglenoid fossa	0.2010
R acromion	0.3984
R infraglenoid fossa	0.2814
L biciptial groove	0.2560
L deltoid tuberosity	0.0000
R bicipital groove	0.2118
R deltoid tuberosity	0.2010
L epicondyle	-0.2471
R epicondyle	0.3163
L olecronon	0.1908
R olecronon	-0.1227

L radial tuberosity	-0.0920
R radial tuberosity	-0.0598
L ilium	0.3583
R ilium	0.3389
L greater troch	-0.0537
L lesser troch	0.1286
L linea aspera	0.3371
R greater troch	0.0704
R lesser troch	-0.3122
R linea aspera	0.3309
L patella	0.1094
R patella	0.1399
L soleal	0.2068
L spine	0.2814
R soleal	0.2010
R spine	-0.0070
L sup calcaneus	-0.1171
L infer calcaneus	0.1902
R sup calcaneus	0.2325
R infer calcaneus	-0.3286

Moderate/severe males: spinal and extraspinal correlations with age

Variable	Age r =
Age	1.0000
length	0.1092
width	0.3217
thick	0.1495
depth	0.2800
vol thick	0.1836
vol depth	0.2023
L acromion	0.3684
L infraglenoid fossa	0.3532
R acromion	0.2406
R infraglenoid fossa	0.6285
L bicip groove	0.1705
L deltoid tub	-0.0721
R bicip groove	0.0521
R deltoid tub	0.2220
L epicondyle	-0.0063
R epicondyle	-0.0894
L olecronon	-0.2110
R olecronon	-0.0500

L radial tub	0.0301
R radial tub	0.2059
L ilium	0.1561
R ilium	0.2577
L Great trochanter	-0.2358
L less trochanter	0.0825
L linea aspera	-0.2236
R greater trochanter	0.5408
R less trochanter	0.2131
R linea aspera	-0.0110
L patella	-0.1860
R patella	-0.1981
L soleal	0.0797
L spine	0.4611
R soleal	-0.1681
R spine	0.0610
L sup calcaneus	0.2665
L infer calcaneus	-0.3171
R sup calcaneus	0.1245
R infer calcaneus	0.2278

APPENDIX III

BILATERALITY: LEFT ELEMENTS CORRELATED WITH RIGHT ELEMENTS

All degrees of DISH pooled males and females: left elements correlated with right elements

Bone	Location	r value
Scapula	Acromion	0.4913
Scapula	Infraglenoid Fossa	0.3699
Humerus	Bicipital Groove	0.6888
Humerus	Deltoid Tuberosity	0.9806
Humerus	Medial Epicondyle	0.4695
Ulna	Olecranon	0.6837
Radius	Radial Tuberosity	0.4175
Ilium	Iliac Crest	0.4849
Femur	Greater Trochanter	0.0847
Femur	Lesser Trochanter	0.7708
Femur	Linea Aspera	0.5223
Patella	Anterior Patella	0.9169
Tibia	Tibial Spines	0.2449
Tibia	Soleal Line	0.4747
Calcaneus	Superior	0.5792
Calcaneus	Inferior	0.0701

All degrees of DISH pooled males only: left elements correlated with right elements

Bone	Location	r value
Scapula	Acromion	0.2073
Scapula	Infraglenoid Fossa	0.1833
Humerus	Bicipital Groove	0.9428
Humerus	Deltoid Tuberosity	-0.0569
Humerus	Medial Epicondyle	0.5996
Ulna	Olecranon	0.6710
Radius	Radial Tuberosity	0.4571
Ilium	Iliac Crest	0.4693
Femur	Greater Trochanter	0.0842
Femur	Lesser Trochanter	0.8148
Femur	Linea Aspera	0.6057
Patella	Anterior Patella	0.7024
Tibia	Tibial Spines	0.0094
Tibia	Soleal Line	0.0744
Calcaneus	Superior	0.3385
Calcaneus	Inferior	-0.0220

All degrees of DISH pooled females only: left elements correlated with right elements

Bone	Location	r value
Scapula	Acromion	0.6624
Scapula	Infraglenoid Fossa	0.3290
Humerus	Bicipital Groove	0.9276
Humerus	Deltoid Tuberosity	0.9828
Humerus	Medial Epicondyle	0.4291
Ulna	Olecranon	0.9633
Radius	Radial Tuberosity	0.1346
Ilium	Iliac Crest	0.7694
Femur	Greater Trochanter	0.2966
Femur	Lesser Trochanter	0.1522
Femur	Linea Aspera	0.1690
Patella	Anterior Patella	0.9934
Tibia	Tibial Spines	0.7302
Tibia	Soleal Line	0.8137
Calcaneus	Superior	0.6642
Calcaneus	Inferior	0.6015

Incipient/mild males and females: left elements correlated with right elements

Bone	Location	r value
Scapula	Acromion	0.1216
Scapula	Infraglenoid Fossa	0.0881
Humerus	Bicipital Groove	0.8295
Humerus	Deltoid Tuberosity	0.8912
Humerus	Medial Epicondyle	0.8601
Ulna	Olecranon	0.7351
Radius	Radial Tuberosity	0.5685
Ilium	Iliac Crest	0.9530
Femur	Greater Trochanter	0.0531
Femur	Lesser Trochanter	0.0421
Femur	Linea Aspera	0.2275
Patella	Anterior Patella	0.9877
Tibia	Tibial Spines	0.6120
Tibia	Soleal Line	0.9811
Calcaneus	Superior	0.3285
Calcaneus	Inferior	0.5952

Incipient/mild males only: left elements correlated with right elements

Bone	Location	r value
Scapula	Acromion	0.1624
Scapula	Infraglenoid Fossa	0.0556
Humerus	Bicipital Groove	0.1902
Humerus	Deltoid Tuberosity	0.0000
Humerus	Medial Epicondyle	0.2087
Ulna	Olecranon	0.5930
Radius	Radial Tuberosity	0.6092
Ilium	Iliac Crest	0.9662
Femur	Greater Trochanter	-0.0760
Femur	Lesser Trochanter	0.0231
Femur	Linea Aspera	0.9990
Patella	Anterior Patella	0.7841
Tibia	Tibial Spines	0.2108
Tibia	Soleal Line	0.9984
Calcaneus	Superior	0.3482
Calcaneus	Inferior	0.1452

Incipient/mild females only: left elements correlated with right elements

Bone	Location	r value
Scapula	Acromion	-0.0514
Scapula	Infraglenoid Fossa	-0.2823
Humerus	Bicipital Groove	0.9999
Humerus	Deltoid Tuberosity	1.0000
Humerus	Medial Epicondyle	0.9753
Ulna	Olecranon	0.9998
Radius	Radial Tuberosity	0.3321
Ilium	Iliac Crest	0.6162
Femur	Greater Trochanter	-0.1246
Femur	Lesser Trochanter	0.7465
Femur	Linea Aspera	0.2241
Patella	Anterior Patella	0.9993
Tibia	Tibial Spines	0.6452
Tibia	Soleal Line	0.7810
Calcaneus	Superior	0.0523
Calcaneus	Inferior	0.5174

Moderate/severe males and females: left elements correlated with right elements

Bone	Location	r value
Scapula	Acromion	0.7384
Scapula	Infraglenoid Fossa	0.8805
Humerus	Bicipital Groove	0.6936
Humerus	Deltoid Tuberosity	0.9972
Humerus	Medial Epicondyle	0.3908
Ulna	Olecranon	0.7619
Radius	Radial Tuberosity	0.3629
Ilium	Iliac Crest	0.4824
Femur	Greater Trochanter	0.0771
Femur	Lesser Trochanter	0.8966
Femur	Linea Aspera	0.5909
Patella	Anterior Patella	0.8480
Tibia	Tibial Spines	0.2253
Tibia	Soleal Line	0.4347
Calcaneus	Superior	0.8753
Calcaneus	Inferior	-0.0454

Moderate/severe males only: left elements correlated with right elements

Bone	Location	r value
Scapula	Acromion	0.5196
Scapula	Infraglenoid Fossa	0.1620
Humerus	Bicipital Groove	0.9754
Humerus	Deltoid Tuberosity	-0.0966
Humerus	Medial Epicondyle	0.6374
Ulna	Olecranon	0.7780
Radius	Radial Tuberosity	0.3889
Ilium	Iliac Crest	0.4601
Femur	Greater Trochanter	0.0536
Femur	Lesser Trochanter	0.9564
Femur	Linea Aspera	0.5737
Patella	Anterior Patella	0.6875
Tibia	Tibial Spines	-0.0297
Tibia	Soleal Line	0.2184
Calcaneus	Superior	0.6703
Calcaneus	Inferior	-0.0687

Moderate/severe females only: left elements correlated with right elements

Bone	Location	r value
Scapula	Acromion	0.7358
Scapula	Infraglenoid Fossa	0.9933
Humerus	Bicipital Groove	0.9997
Humerus	Deltoid Tuberosity	1.0000
Humerus	Medial Epicondyle	0.3085
Ulna	Olecranon	0.9839
Radius	Radial Tuberosity	0.0739
Ilium	Iliac Crest	0.8550
Femur	Greater Trochanter	0.9094
Femur	Lesser Trochanter	0.1115
Femur	Linea Aspera	0.8191
Patella	Anterior Patella	0.9964
Tibia	Tibial Spines	0.7740
Tibia	Soleal Line	0.8756
Calcaneus	Superior	0.8999
Calcaneus	Inferior	0.4441

NOTE TO USERS

Page(s) not included in the original manuscript and are unavailable from the author or university. The manuscript was scanned as received.

missing vita page 127

This reproduction is the best copy available.

UMI®